



Estimation of rate coefficients and branching ratios for gas-phase reactions of OH with aromatic organic compounds for use in automated mechanism construction

Michael E. Jenkin^{1,2}, Richard Valorso³, Bernard Aumont³, Andrew R. Rickard^{4,5}, and Timothy J. Wallington⁶

¹Atmospheric Chemistry Services, Okehampton, Devon, EX20 4QB, UK

²School of Chemistry, University of Bristol, Cantock's Close, Bristol, BS8 1TS, UK

³LISA, UMR CNRS 7583, Université Paris Est Créteil et Université Paris Diderot, Institut Pierre Simon Laplace, 94010 Créteil, France

⁴Wolfson Atmospheric Chemistry Laboratories, Department of Chemistry, University of York, York, YO10 5DD, UK

⁵National Centre for Atmospheric Science, University of York, York, YO10 5DD, UK

⁶Research and Advanced Engineering, Ford Motor Company, SRL-3083, P.O. Box 2053, Dearborn, MI 48121-2053, USA

Correspondence: Michael E. Jenkin (atmos.chem@btinternet.com)

Received: 6 February 2018 – Discussion started: 19 February 2018

Revised: 2 June 2018 – Accepted: 6 June 2018 – Published: 4 July 2018

Abstract. Reaction with the hydroxyl (OH) radical is the dominant removal process for volatile organic compounds (VOCs) in the atmosphere. Rate coefficients for the reactions of OH with VOCs are therefore essential parameters for chemical mechanisms used in chemistry transport models, and are required more generally for impact assessments involving estimation of atmospheric lifetimes or oxidation rates for VOCs. A structure–activity relationship (SAR) method is presented for the reactions of OH with aromatic organic compounds, with the reactions of aliphatic organic compounds considered in the preceding companion paper. The SAR is optimized using a preferred set of data including reactions of OH with 67 monocyclic aromatic hydrocarbons and oxygenated organic compounds. In each case, the rate coefficient is defined in terms of a summation of partial rate coefficients for H abstraction or OH addition at each relevant site in the given organic compound, so that the attack distribution is defined. The SAR can therefore guide the representation of the OH reactions in the next generation of explicit detailed chemical mechanisms. Rules governing the representation of the reactions of the product radicals under tropospheric conditions are also summarized, specifically the rapid reaction sequences initiated by their reactions with O₂.

1 Introduction

Aromatic hydrocarbons make a significant contribution to anthropogenic emissions of volatile organic compounds (VOCs), representing an important component of vehicle exhaust and other combustion emissions, and evaporative emissions of petroleum and from industrial processes and solvent usage (e.g. Calvert et al., 2002; Passant, 2002). They are also emitted from sources that are either partially or wholly natural. They represent a significant proportion of VOC emissions from biomass burning sources (e.g. Hays et al., 2002; Lewis et al., 2013), and are emitted substantially from vegetation (e.g. Misztal et al., 2015). An important contributor to these natural emissions is *p*-cymene (e.g. Helmig et al., 1998; Owen et al., 2001; Maleknia et al., 2007; Ulman et al., 2007), which is also formed as a degradation product of the reactive monoterpenes α -terpinene, α -phellandrene and γ -phellandrene (e.g. Berndt et al., 1996; Peeters et al., 1999; Aschmann et al., 2011). The aromatic oxygenate, methyl chavicol (1-allyl-4-methoxybenzene), has also been reported to be emitted in large quantities from vegetation (Bouvier-Brown et al., 2009; Misztal et al., 2010), with evidence for a number of other aromatic oxygenates also reported (Misztal et al., 2015). It is well established that the gas-phase degradation of VOCs in general plays a central role in the generation of a variety of secondary pollutants, including ozone and

secondary organic aerosol, SOA (e.g. Haagen-Smit and Fox, 1954; Went, 1960; Andreae and Crutzen, 1997; Jenkin and Clemitshaw, 2000; Hallquist et al., 2009). By virtue of their generally high reactivity and emissions, the oxidation of aromatic compounds is believed to make an important contribution to the formation of ozone on local and regional scales (Derwent et al., 1996; Calvert et al., 2002), and to the formation of SOA in urban areas (e.g. Odum et al., 1997; Genter et al., 2017).

The complete gas-phase oxidation of aromatic hydrocarbons proceeds via highly detailed mechanisms, producing a variety of intermediate oxidized organic products, some of which retain the aromatic ring (e.g. Calvert et al., 2002; Jenkin et al., 2003; Bloss et al., 2005). Reaction with the hydroxyl (OH) radical is generally the dominant or exclusive removal process for aromatic hydrocarbons, and makes a major contribution to the removal of aromatic oxygenates. Quantified rate coefficients for these reactions are therefore essential parameters for chemical mechanisms used in chemistry transport models, and are required more generally for environmental assessments of their impacts, e.g. to estimate the kinetic component of ozone formation potentials (Jenkin et al., 2017). In addition to the total rate coefficient, quantification of the branching ratio for attack of OH at each site within a given compound is required for explicit representation of the subsequent oxidation pathways in chemical mechanisms.

In the present paper, a structure–activity relationship (SAR) method is presented for the reactions of OH with aromatic organic compounds, with the reactions of aliphatic organic compounds considered in the preceding companion paper (Jenkin et al., 2018a). In each case, the rate coefficient is defined in terms of a summation of partial rate coefficients for H-atom abstraction or OH addition at each relevant site in the given organic compound, so that the attack distribution is also defined. This is therefore the first generalizable SAR for reactions of OH with aromatic compounds that aims to capture observed trends in rate coefficients and the site-specificity of attack. Application of the methods is illustrated with examples in the Supplement.

The information is currently being used to guide the representation of the OH-initiation reactions in the next generation of explicit detailed chemical mechanisms, based on the Generator for Explicit Chemistry and Kinetics of Organics in the Atmosphere (GECKO-A; Aumont et al., 2005), and the Master Chemical Mechanism (MCM; Saunders et al., 2003). It therefore contributes to a revised and updated set of rules that can be used in automated mechanism construction, and provides formal documentation of the methods. To facilitate this, rules governing the representation of the reactions of the product radicals under tropospheric conditions are also summarized, specifically the rapid reaction sequences initiated by their reactions with O₂. The subsequent chemistry (e.g. reactions of peroxy radicals) will be considered elsewhere (Jenkin et al., 2018b).

2 Preferred kinetic data

A set of preferred kinetic data has been assembled from which to develop and validate the estimation methods for the OH rate coefficients, as described in the companion paper (Jenkin et al., 2018a). The subset relevant to the present paper comprises 298 K data for 25 monocyclic aromatic hydrocarbons (with temperature dependences also defined in 13 cases) and 42 aromatic oxygenated organic compounds (with temperature dependences also defined in 7 cases). In one case (1,2-diacetylbenzene), the preferred rate coefficient is an upper-limit value. The information is provided as a part of the Supplement (as identified in spreadsheets SI_6 and SI_7). As described in more detail in Sect. 3.2, the oxygenates include compounds containing a variety of oxygenated substituent groups that are prevalent in both emitted VOCs and their degradation products, namely -OH, -C(OH)<, -C(=O)-, -O-, -C(=O)O- and -NO₂ groups. For a core set of 11 reactions, the preferred kinetic data are based on the evaluations of the IUPAC Task Group on Atmospheric Chemical Kinetic Data Evaluation (<http://iupac.pole-ether.fr/>; last access: September 2017). The remaining values are informed by recommendations from other key evaluations with complementary coverage (e.g. Atkinson and Arey, 2003; Calvert et al., 2011), and have been revised and expanded following review and evaluation of additional data not included in those studies (as identified in spreadsheets SI_6 and SI_7).

3 Kinetics and branching ratios of initiation reactions

The reaction of OH with a given aromatic compound can occur by both addition of OH to the aromatic ring and by abstraction of an H atom from a C-H or O-H bond in a substituent group. The estimated rate coefficient is therefore given by $k_{\text{calc}} = k_{\text{add}} + k_{\text{abs}}$, where k_{add} and k_{abs} are summations of the partial rate coefficients for OH addition and H-atom abstraction for each attack position in the given aromatic compound. Based on reported data for the reaction of OH with benzene, abstraction of H atoms from the aromatic ring itself is assumed to be negligible under atmospheric conditions (e.g. see Calvert et al., 2002).

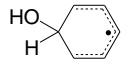
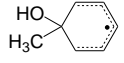
A method for estimating rate coefficients for OH addition to the aromatic ring (k_{add}), and the distribution of attack, is described in the sections that follow. The estimation of rate coefficients for H-atom abstraction from substituent groups (k_{abs}) follows the methods described in the companion paper (Jenkin et al., 2018a), which are mainly based on updating and extending the widely applied method of Kwok and Atkinson (1995). For C-H bonds, the estimated rate coefficients are thus generally based on a summation of rate coefficients for H-atom abstraction from the primary (-CH₃), secondary (-CH₂-) and tertiary (-CH<) groups which are calculated as follows:

Table 1. Neighbouring group factors, $F(X)$, for α -H-atom abstraction from substituents in aromatics, and their temperature dependences described by $F(X) = A_{F(X)} \exp(-B_{F(X)}/T)$.

Substituent	Parameter	$A_{F(X)}$	$B_{F(X)}$ (K)	$F(X)_{298\text{ K}}$	Comment
$-\text{CH}_3$, $-\text{CH}_2\text{OX}$	$F(-\text{Ph1})$	8.6	345	2.7	a,b
$-\text{CH}_2-$, $-\text{CH}<$	$F(-\text{Ph2})$	7.0	580	1.0	a,c

Comments: ^a the value of $F(\text{Ph1})$ or $F(\text{Ph2})$ should be further scaled by the factor “ $\exp(140/T)$ ” for each alkyl group positioned *ortho* or *para* to the abstraction group. ^b Applies to H-atom abstraction from CH_3 and CH_2OX substituents. Value of $F(-\text{Ph1})$ is assigned so that $k_{\text{prim}} \cdot F(-\text{Ph1})$ equals the recommended H-atom abstraction rate coefficient for the methyl group in toluene, i.e. $2.5 \times 10^{-11} \exp(-1270/T) \text{ cm}^3 \text{ molecule}^{-1} \text{ s}^{-1}$ (IUPAC, 2017a); $F(-\text{Ph1})$ value is also consistent with reported abstraction from the $-\text{CH}_2\text{OH}$ substituent in benzyl alcohol (Harrison and Wells, 2009; Bernard et al., 2013) and is therefore applied to $-\text{CH}_2\text{OX}$ groups in general, where $-\text{OX}$ denotes the oxygenated groups $-\text{OH}$, $-\text{OR}$, $-\text{OOH}$, $-\text{OOR}$ and $-\text{ONO}_2$. ^c Applies to H-atom abstraction from secondary ($-\text{CH}_2-$) and tertiary ($-\text{CH}<$) groups in $\geq \text{C}_2$ substituents. Value of $F(-\text{Ph2})$ is assigned on the basis of the reported contribution of H-atom abstraction from the *i*-propyl group in *p*-cymene (Aschmann et al., 2010; Bedjanian et al., 2015).

Table 2. Group rate coefficients for OH addition to carbon atoms in monocyclic aromatic rings, and their temperature dependences described by $k = A \exp(-(E/R)/T)$. Parameters are shown for addition to an unsubstituted carbon (k_{arom}) and to a methyl-substituted carbon (k_{ipso}).

Product radical	Parameter	A ($10^{-12} \text{ cm}^3 \text{ molecule}^{-1} \text{ s}^{-1}$)	E/R (K)	$k_{298\text{ K}}$ ($10^{-12} \text{ cm}^3 \text{ molecule}^{-1} \text{ s}^{-1}$)	Comment
	k_{arom}	0.378	190	0.20	a
	k_{ipso}	0.378	89	0.28	b

Comments: ^a by definition, k_{arom} is 1/6 of the preferred rate coefficient for the reaction of OH with benzene. ^b k_{ipso} at 298 K optimized in conjunction with substituent factors in Table 3, using preferred kinetic data for 12 methyl-substituted aromatic hydrocarbons. The assigned temperature dependence adopts the value of A for k_{arom} , with E/R adjusted to return the optimized value of k_{ipso} at 298 K.

$$k(\text{CH}_3\text{-X}) = k_{\text{prim}} F(X), \quad (1)$$

$$k(\text{X-CH}_2\text{-Y}) = k_{\text{sec}} F(X) F(Y), \quad (2)$$

$$k(\text{X-CH(-Y)-Z}) = k_{\text{tert}} F(X) F(Y) F(Z), \quad (3)$$

where k_{prim} , k_{sec} and k_{tert} are the respective group rate coefficients for abstraction from primary, secondary and tertiary groups for a reference substituent; and $F(X)$, $F(Y)$ and $F(Z)$ are factors that account for the effects of the substituents X, Y and Z. The reference substituent is defined as “ $-\text{CH}_3$ ”, such that $F(-\text{CH}_3) = 1.00$ (Atkinson, 1987; Kwok and Atkinson, 1995). As described in detail in the companion paper (Jenkin et al., 2018a), a number of fixed rate coefficients are also defined for H-atom abstraction from O-H bonds in hydroxy, hydroperoxy and carboxyl groups; and for C-H bonds in a series of formyl groups, and adjacent to $-\text{O}-$ linkages in ethers. The values of these rate coefficients are assumed to be independent of the identity of neighbouring substituent groups. The methods summarized above are extended in the present work to include rate coefficients and neighbouring group substituent factors for H-atom abstraction from carbon and oxygen atoms adjacent to aromatic rings.

For aromatic compounds containing an unsaturated substituent, the addition of OH to $\text{C}=\text{C}$ bonds in the substituent group can also occur. The treatment of these reactions is described in Sect. 3.1.3.

3.1 Aromatic hydrocarbons

3.1.1 Methyl-substituted aromatic hydrocarbons

The set of preferred kinetic data contains rate coefficients for the reactions of OH with 12 methyl-substituted aromatic hydrocarbons possessing between one and six methyl substituents. This class is the most comprehensively studied, with room temperature data covering all possible methyl-substituted isomers. Although rate coefficients for this class of compound do not therefore need to be estimated, the SAR described below aims to rationalize the variation of reactivity from one compound to another, and to provide a method of estimating the OH attack distributions that can be applied in automated mechanism generation.

The contribution of H-atom abstraction to the total rate coefficient is known to be minor at temperatures relevant to the atmosphere for methyl-substituted aromatics (e.g. Calvert et al., 2002; Loison et al., 2012; Aschmann et al., 2013). The temperature-dependent reference substituent factor for a phenyl group, $F(-\text{Ph1})$ (see Table 1), was set so that the H-atom abstraction rate coefficient for the methyl group in toluene matches the IUPAC recommendation, i.e. $2.5 \times 10^{-11} \exp(-1270/T) \text{ cm}^3 \text{ molecule}^{-1} \text{ s}^{-1}$ (IUPAC, 2017a). The branching ratios reported in the above

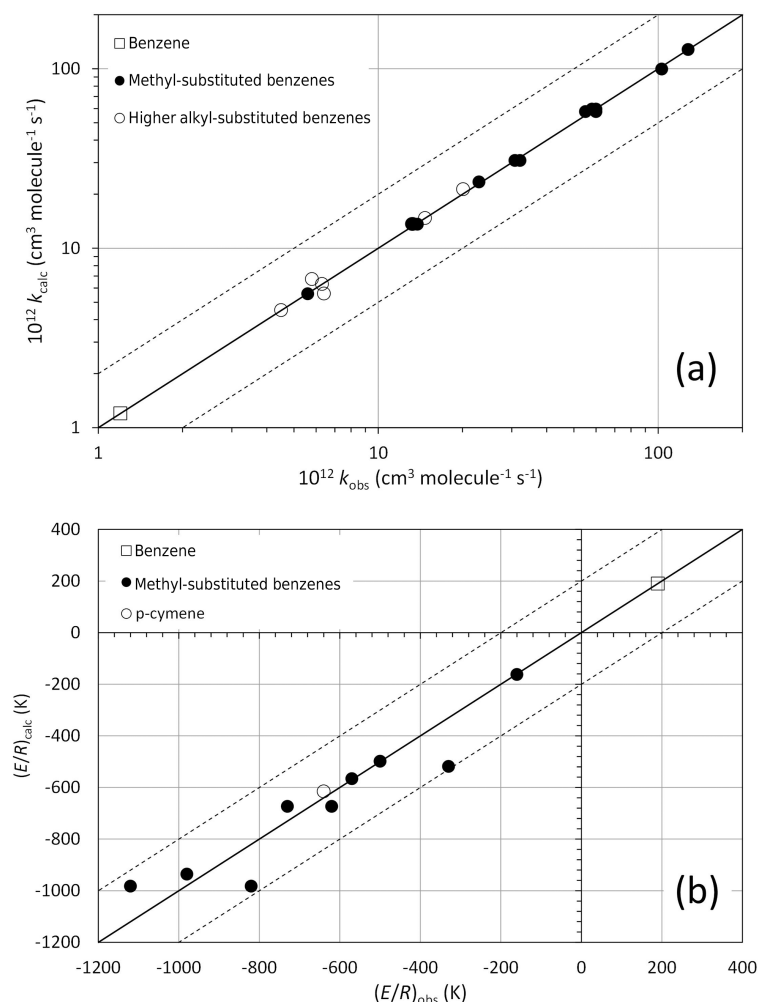


Figure 1. (a) A log–log correlation of k_{calc} and k_{obs} at 298 K for benzene, methyl-substituted benzenes and higher alkyl-substituted benzenes. The broken lines show the factor of 2 range. (b) A correlation of the temperature coefficients $(E/R)_{\text{calc}}$ and $(E/R)_{\text{obs}}$ for the same compound classes. The broken lines show the ± 200 K range.

studies suggest that H-atom abstraction is slightly more efficient for methyl groups in some polymethyl-substituted aromatics, particularly for hexamethylbenzene (Loison et al., 2012), probably reflecting an additional stabilizing effect on the resonant product radical. The data were thus found to be reasonably well described by assigning a further activation factor of $\exp(140/T)$ (equating to a value of 1.6 at 298 K) for each additional methyl group positioned *ortho* or *para* to the abstraction group. The resultant estimated branching ratios for H-atom abstraction are discussed further below.

The current estimation method defines site-specific parameters for addition of OH to each carbon atom in the aromatic ring. As shown in Table 2, k_{arom} is used to represent addition of OH to an unsubstituted carbon, and k_{ipso} is used to represent addition of OH to a methyl-substituted carbon. The total rate coefficient for OH addition is then given by a summation of the partial rate coefficients for each of the six attack positions,

$$k_{\text{add}} = \sum k F(\Phi), \quad (4)$$

where k is either k_{arom} or k_{ipso} and $F(\Phi)$ is a factor that accounts for the effect of the combination of methyl substituents in the molecule in terms of their positions (i.e. *ortho*, *meta* or *para*) relative to each OH addition location.

As shown in Table 3, the dataset was described in terms of 11 substituent factors, representing the effects of between one and five methyl substituents. Based on the results of previous assessments (e.g. see Calvert et al., 2002), the number of parameters was limited by assuming that *ortho* and *para* substituents have the same influence, whether individually or in combinations. Examples of rate coefficient calculations using these parameters are given in the Supplement.

The values of the $F(\Phi)$ factors in Table 3 and k_{ipso} were varied iteratively to minimize the summed square deviation, $\Sigma((k_{\text{calc}} - k_{\text{obs}}) / k_{\text{obs}})^2$ at 298 K for the set of methyl-

Table 3. Substituent factors $F(\Phi)$ for the addition reactions of OH to aromatic hydrocarbons, and their temperature dependences described by $F(\Phi) = A_{F(\Phi)} \exp(-B_{F(\Phi)}/T)$. Each factor relates to the combination of methyl substitutions indicated relative to the OH attack position (*o* = *ortho*-, *m* = *meta*-, *p* = *para*-).

Number of substituents	Parameter	$A_{F(\Phi)}$	$B_{F(\Phi)}$	$F(\Phi)_{298\text{ K}}$	Comment
1	$F(o-), F(p-)$	0.8	−659	7.3	a
	$F(m-)$	0.7	−207	1.4	b
2	$F(o-, o-), F(o-, p-)$	0.6	−1203	34	c
	$F(o-, m-), F(m-, p-)$	2.6	−416	10.5	d
	$F(m-, m-)$	1.9	−409	7.5	e
	$F(o-, o-, p-)$	6.8	−760	87	f
3	$F(o-, o-, m-), F(o-, m-, p-)$	0.5	−1200	28	g
	$F(o-, m-, m-), F(m-, m-, p-)$	3.5	−341	11	h
	$F(o-, o-, m-, p-)$	2.0	−998	57	i
4	$F(o-, o-, m-, m-), F(o-, m-, m-, p-)$	0.3	−1564	57	j
	$F(o-, o-, m-, m-, p-)$	4.7	−809	71	k

Comments: given parameter contributes to the calculation of k_{calc} for the following methyl-substituted aromatics: ^a toluene, *o*-xylene and *p*-xylene; ^b toluene and *m*-xylene; ^c *m*-xylene, 1,2,3-trimethylbenzene and 1,2,4-trimethylbenzene; ^d *o*-xylene, *p*-xylene, 1,2,3-trimethylbenzene and 1,2,4-trimethylbenzene; ^e *m*-xylene and 1,3,5-trimethylbenzene; ^f 1,3,5-trimethylbenzene and 1,2,3,5-tetramethylbenzene; ^g 1,2,3-trimethylbenzene, 1,2,4-trimethylbenzene, 1,2,3,4-tetramethylbenzene, 1,2,3,5-tetramethylbenzene and 1,2,4,5-tetramethylbenzene; ^h 1,2,3-trimethylbenzene, 1,2,4-trimethylbenzene and 1,2,3,5-tetramethylbenzene; ⁱ 1,2,3,5-tetramethylbenzene and pentamethylbenzene; ^j 1,2,3,4-tetramethylbenzene, 1,2,4,5-tetramethylbenzene and pentamethylbenzene; ^k pentamethylbenzene and hexamethylbenzene.

Table 4. Comparison of estimated and reported branching ratios for H-atom abstraction, $k_{\text{abs}}/(k_{\text{abs}} + k_{\text{add}})$, at 298 K except where indicated.

Compound	Branching ratio		Comment
	Calculated	Observed	
toluene	6.3 %	6.3 %	a
<i>o</i> -xylene	8.3 %	~ 10 %	b
<i>m</i> -xylene	3.0 %	~ 4 %	b
<i>p</i> -xylene	8.3 %	~ 7–8 %	b
1,2,4,5-tetramethylbenzene	6.2 %	(3.7 ± 0.8) %	c
hexamethylbenzene	10.8 %	(13.7 ± 4.4) %	d
<i>p</i> -cymene (total)	22.4 %	(20 ± 4) %	e
<i>p</i> -cymene (at >CH-)	16.2 %	(14.8 ± 3.2) %	e

Comments: sources of observed values: ^a Based on the recommendation of the IUPAC Task Group on Atmospheric Chemical Kinetic Data Evaluation (IUPAC, 2017a). ^b Calvert et al. (2002). ^c Aschmann et al. (2013). ^d Loison et al. (2012), measurement at 330 K. ^e Taken from Aschmann et al. (2010). Total branching ratio is also consistent with data of Bedjanian et al. (2015)

substituted aromatic hydrocarbons. Within the context of previous appraisals (e.g. Calvert et al., 2002 and references therein), the resultant values show some consistent trends, with *ortho* and *para* substituents being significantly more activating than *meta* substituents. It is also interesting to note that the elevation in k_{ipso} relative to k_{arom} (i.e. a factor of 1.4) is identical to the activating influence of a lone *meta* substituent, which is also consistent with previous assumptions (e.g. Calvert et al., 2002). Increasing the number of substituents has a generally increasing activating impact, although the highest value was returned for $F(o-, o-, p-)$, i.e. for three substituents in the most activating positions, with this value being determined by the observed rate coefficients

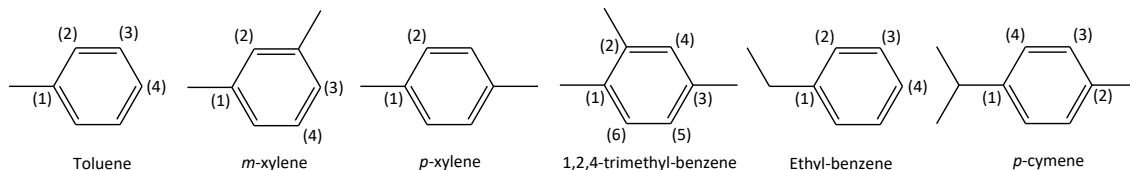
for 1,3,5-trimethylbenzene and 1,2,3,5-tetramethylbenzene. A correlation of the optimized values of k_{calc} with k_{obs} at 298 K is shown in Fig. 1. The estimation method reproduces all the observed values to within 5 %.

The estimated contributions of H-atom abstraction from the methyl substituents in the series of aromatic hydrocarbons are compared with those reported in Table 4. The values confirm that rate coefficients assigned to these reactions in Table 1 provide a reasonable description for the complete dataset of methyl-substituted aromatics.

There have been no direct experimental determinations of the branching ratios for OH addition to methyl-substituted aromatic rings, although a number of density functional the-

Table 5. Comparison of estimated branching ratios for OH addition to alkyl-substituted aromatic hydrocarbons at 298 K with those reported in density functional theory (DFT) studies. Displayed values are presented relative to k_{add} .

Addition site	Degeneracy	Branching ratios		
1. toluene		this work	Suh et al. (2002)	Wu et al. (2014) ^a
<i>ipso</i> - (1)	1	5.4 %	3 %	16.1 %
<i>ortho</i> - (2)	2	55.9 %	52 %	63.4 %
<i>meta</i> - (3)	2	10.7 %	11 %	5.4 %
<i>para</i> - (4)	1	28.0 %	34 %	15.1 %
2. <i>m</i> -xylene		this work	Fan et al. (2008)	Huang et al. (2011) ^b
<i>ipso</i> -, <i>meta</i> - (1)	2	3.5 %	1 %	1.9 %
<i>ortho</i> -, <i>ortho</i> - (2)	1	30.0 %	60 %	60.7 %
<i>ortho</i> -, <i>para</i> - (3)	2	60.0 %	37 %	28.3 %
<i>meta</i> -, <i>meta</i> - (4)	1	6.6 %	2 %	9.1 %
3. <i>p</i> -xylene		this work	Fan et al. (2006)	
<i>ipso</i> -, <i>para</i> - (1)	2	32.7 %	20 %	
<i>ortho</i> -, <i>meta</i> - (2)	4	67.3 %	80 %	
4. 1,2,4-trimethylbenzene		this work	Li et al. (2014) ^c	
<i>ipso</i> -, <i>ortho</i> -, <i>para</i> - (1)	1	33.1 %	23.4 %	
<i>ipso</i> -, <i>ortho</i> -, <i>meta</i> - (2)	1	10.2 %	8.5 %	
<i>ipso</i> -, <i>meta</i> -, <i>para</i> - (3)	1	10.2 %	5.3 %	
<i>ortho</i> -, <i>ortho</i> -, <i>meta</i> - (4)	1	19.4 %	20.2 %	
<i>ortho</i> -, <i>meta</i> -, <i>para</i> - (5)	1	19.4 %	40.4 %	
<i>ortho</i> -, <i>meta</i> -, <i>meta</i> - (6)	1	7.6 %	2.1 %	
5. ethylbenzene		this work	Huang et al. (2010)	
<i>ipso</i> - (1)	1	5.6 %	6 %	
<i>ortho</i> - (2)	2	56.0 %	53 %	
<i>meta</i> - (3)	2	10.4 %	10 %	
<i>para</i> - (4)	1	28.0 %	31 %	
6. <i>p</i> -cymene		this work	Alarcón et al. (2014)	
<i>ipso</i> -, <i>para</i> - (1)	1	17.9 %	18 %	
<i>ipso</i> -, <i>para</i> - (2)	1	14.8 %	3 %	
<i>ortho</i> -, <i>meta</i> - (3)	2	36.8 %	24 %	
<i>ortho</i> -, <i>meta</i> - (4)	2	30.5 %	55 %	



Comments: ^a values given relative to $k_{\text{add}} + k_{\text{abs}}$ in Wu et al. (2014), as 15, 59, 5 and 14 %. ^b Values given relative to $k_{\text{add}} + k_{\text{abs}}$ in Huang et al. (2011), as 1.9, 60, 28 and 9 %. ^c Values given relative to $k_{\text{add}} + k_{\text{abs}}$ in Li et al. (2014) as 22, 8, 5, 19, 38 and 2 %.

ory (DFT) studies have been reported for toluene, *m*-xylene, *p*-xylene and 1,2,4-trimethylbenzene (Suh et al., 2002; Fan et al., 2006; 2008; Huang et al., 2011; Wu et al., 2014; Li et al., 2014). As shown in Table 5, the attack distributions of OH predicted by the partial rate coefficients determined from the present method are generally consistent with those reported in the theoretical studies, providing a level of independent support for the method developed here. The distributions for toluene and *p*-xylene are in good agreement with those reported in the DFT studies, with those for 1,2,4-trimethyl ben-

zene also being in reasonable agreement. For *m*-xylene, the major channels (i.e. addition at positions 2 and 3) are consistent with those reported by Fan et al. (2008) and Huang et al. (2011), although their relative importance is reversed. The present method predicts addition at position (3) to be more important because of its greater degeneracy, whereas the DFT studies predict that this is outweighed by a much stronger activating influence of the two *ortho* substitutions on position (2) compared with that of the *ortho* and *para* substitutions on position (3). Conversely, the opposite appears to

be the case for 1,2,4-trimethyl benzene, where the DFT study of Li et al. (2014) calculates position (5) (with *ortho* and *para* substitutions) to be favoured over position (4) (with two *ortho* substitutions), despite both sites being singly degenerate in that case.

Temperature-dependent recommendations are available for benzene and 10 methyl-substituted aromatics in Arrhenius format ($k = A \exp(-(E/R)/T)$) (see spreadsheet SI_6). These were used to provide optimized temperature coefficients ($B_{F(\Phi)}$) and pre-exponential factors ($A_{F(\Phi)}$) for the set of OH addition substituent factors given in Table 3. Optimization was achieved by calculating values of k at even $1/T$ intervals over the recommended temperature range for each aromatic, and determining a composite E/R value from a least squares linear regression of the data on an Arrhenius (i.e. $\ln(k)$ vs. $1/T$) plot. The 11 values of $B_{F(\Phi)}$ in Table 3 were varied to minimize the summed square deviation in the composite temperature coefficients, $\Sigma((E/R)_{\text{calc}} - (E/R)_{\text{obs}})^2$. The resultant $(E/R)_{\text{calc}}$ values are compared with the recommended $(E/R)_{\text{obs}}$ values in the lower panel of Fig. 1 (see also Fig. S1 in the Supplement). The values of $A_{F(\Phi)}$ were automatically returned from the corresponding optimized $B_{F(\Phi)}$ and $F(\Phi)_{298\text{ K}}$ values.

3.1.2 Higher alkyl-substituted aromatic hydrocarbons

The set of preferred kinetic data contains rate coefficients for a further eight alkyl-substituted aromatic hydrocarbons, namely ethylbenzene, *n*-propylbenzene, *i*-propylbenzene, *t*-butylbenzene, *o*-ethyltoluene, *m*-ethyltoluene, *p*-ethyltoluene and *p*-cymene. Information on H-atom abstraction from this series of compounds is limited to the study of *p*-cymene (4-*i*-propyltoluene) reported by Aschmann et al. (2010) and Bedjanian et al. (2015), who determined a total branching ratio for H-atom abstraction of about 20 %, with about 15 % from the $-\text{CH}<$ group in the *i*-propyl substituent (see Table 4). Use of the aromatic substituent factors appropriate to H-atom abstraction from $\alpha\text{-CH}_3$ groups (i.e. $F(-\text{Ph}1)$ in Table 1) would clearly lead to a gross overestimation for *p*-cymene (i.e. about 34 % from the $-\text{CH}<$ group in the *i*-propyl substituent and a total of about 39 %), and also unreasonably large contributions in the other compounds identified above. Based on the *p*-cymene data, a substituent factor of 1.0 is assigned to $F(-\text{Ph}2)$, representing H-atom abstraction from a substituent $\alpha\text{-CH}<$ group, and also applied to abstraction from an $\alpha\text{-CH}_2\text{-}$ group in $\geq\text{C}_2$ substituents (see Table 1). As for the $-\text{CH}_3$ groups discussed above, the further activation factor of $\exp(140/T)$ (equating to a value of 1.6 at 298 K) is applied for each additional alkyl group positioned *ortho* or *para* to the abstraction group. For *p*-cymene, this results in an estimated total branching ratio for H-atom abstraction of 22.4 %, with 16.2 % from the $-\text{CH}<$ group in the *i*-propyl substituent (see Table 4), in good agreement with the observations of Aschmann et al. (2010) and Bedjanian et al. (2015). It is noted that the

value of 1.0 assigned to $F(-\text{Ph}2)$ at 298 K is unchanged from that previously reported by Kwok and Atkinson (1995) for phenyl groups in general.

The methyl group substituent factors in Table 3 provide a reasonable first approximation for the effects of the higher alkyl groups on OH addition rate coefficients, and use of those factors leads to a set of estimated rate coefficients that are all within 30 % of the observed values for the current set of eight higher alkyl-substituted aromatic hydrocarbons. On the whole, however, this results in a slight overestimation of the rate coefficients. Table 6 shows a set of adjustment factors for non-methyl substituents, $R(\Phi)$, that represent corrections to the values of $F(\Phi)$ in Table 3 (and to k_{ipso} , when appropriate), such that:

$$k_{\text{add}} = \Sigma k F(\Phi) R(\Phi). \quad (5)$$

These result in a generally improved agreement, with deviations from the observed rate coefficients of $\leq 16\%$ (see Fig. 1). For the present set of compounds, these adjustment factors are only defined for the impacts of *ortho* and *para* substitutions, as adjustments for *meta* and *ipso* groups appeared to result in more subtle benefits. In principle, a value of $R(\Phi)$ should be applied for each higher alkyl group in the molecule, although none of the current set contains more than one higher alkyl substituent. The factors appear to show a deactivating effect (relative to that of methyl) that increases with the size of the alkyl group, with this being qualitatively consistent with information reported in previous appraisals (e.g. see Calvert et al., 2002). It is emphasized, however, that the adjustment factors are derived from the analysis of a very small dataset, with some factors based on reported data for a single compound. Clearly, further systematic kinetic studies of higher alkyl-substituted aromatics would be of benefit.

Similarly to above, there have been no direct experimental determinations of branching ratios for OH addition to higher alkyl-substituted aromatics, although Huang et al. (2010) have reported a DFT study for ethylbenzene, and Alarc3n et al. (2014) for *p*-cymene. As shown in Table 5, the attack distributions of OH predicted by the partial rate coefficients determined from the present method agree reasonably well with those reported.

Temperature-dependent studies are only available for *p*-cymene (Alarc3n et al., 2014; Bedjanian et al., 2015), resulting in a recommended value of $E/R = -640\text{ K}$. The parameters discussed above are unable to recreate this temperature dependence, and logically return a temperature dependence comparable to that of the structurally similar compound *p*-xylene, for which the recommended $E/R = -160\text{ K}$. It was found that this discrepancy could be resolved by applying a temperature dependent value of $R_{i\text{-pr}}(o-) = R_{i\text{-pr}}(p-) = 0.029 \exp(1000/T)$ (see Table 6, comment d). This results in *i*-propyl groups becoming more activating relative to methyl groups as the temperature is lowered, with values of $R_{i\text{-pr}}(o-)$ and $R_{i\text{-pr}}(p-) > 1$ at temperatures below about 280 K. The

Table 6. Substituent adjustment factors, $R(\Phi)$, relative to the $F(\Phi)$ values shown for methyl substituents in Table 3 and k_{ipso} in Table 2. Tabulated values are applicable to 298 K, with suggested temperature dependences provided in the comments^a.

Substituent	Parameter	Position of substituent				Comment
		<i>ortho</i> -	<i>para</i> -	<i>meta</i> -	<i>ipso</i> -	
methyl	–	1.0	1.0	1.0	1.0	b
ethyl	$R_{\text{et}}(\Phi)$	0.87	0.87	1.0	1.0	c
<i>i</i> -propyl	$R_{i\text{-pr}}(\Phi)$	0.83	0.83	1.0	1.0	d
<i>n</i> -propyl	$R_{n\text{-pr}}(\Phi)$	0.83	0.83	1.0	1.0	e
<i>t</i> -butyl	$R_{t\text{-bu}}(\Phi)$	0.72	0.72	1.0	1.0	f
alk-1-enyl (vinyl)	$R_{\text{vinyl}}(\Phi)$	0.0	0.0	0.0	0.0	g
-OH	$R_{\text{OH}}(\Phi)$	2.6	2.6	2.4	2.4	h
-CH ₂ OH, -CH(OH)R, -C(OH)R ₂	$R_{\text{C-OH}}(\Phi)$	3.7	3.7	3.7	3.7	i
-C(=O)H, -C(=O)R	$R_{\text{C(O)H}}(\Phi)$, $R_{\text{C(O)R}}(\Phi)$	0.096	0.096	0.096	0.096	j
-OCH ₃ , -OR	$R_{\text{OMe}}(\Phi)$, $R_{\text{OR}}(\Phi)$	3.4	3.4	0.79	0.79	k
-OC ₆ H ₅	$R_{\text{OPh}}(\Phi)$	0.90	0.90	0.21	0.21	l
-C(=O)OCH ₃ -C(=O)OR	$R_{\text{C(O)OMe}}(\Phi)$, $R_{\text{C(O)OR}}(\Phi)$	0.26	0.26	0.26	0.26	m
-NO ₂ , -ONO ₂	$R_{\text{NO}_2}(\Phi)$	0.024	0.024	0.070	0.070	n

^a Applied to values of $F(\Phi)$ in Table 3 for each component group, and to k_{ipso} . ^b Factors are 1.0 by definition. ^c Based on optimization to data for ethylbenzene, *o*-ethyltoluene, *m*-ethyltoluene and *p*-ethyltoluene. Use of a temperature dependent factor, $R_{\text{et}}(o-) = R_{\text{et}}(p-) = 0.029 \exp(1014/T)$, is provisionally suggested, where the pre-exponential factor is based on that determined for the *i*-propyl group (see comment d). ^d Based on optimization to data for *i*-propylbenzene, and *p*-cymene (4-*i*-propyltoluene). Use of a temperature dependent factor, $R_{i\text{-pr}}(o-) = R_{i\text{-pr}}(p-) = 0.029 \exp(1000/T)$, allows observed preferred temperature dependence of k for *p*-cymene to be recreated (see Sect. 3.1.2). ^e Provisionally assumed equivalent to *i*-propyl group adjustment factor, although a much lower factor (0.62) would recreate the reported k for *n*-propylbenzene. Use of a temperature dependent factor, $R_{n\text{-pr}}(o-) = R_{n\text{-pr}}(p-) = 0.029 \exp(1014/T)$, is provisionally suggested (see comment e). ^f Based on optimization to data for *t*-butylbenzene. Use of a temperature dependent factor, $R_{t\text{-bu}}(o-) = R_{t\text{-bu}}(p-) = 0.029 \exp(957/T)$, is provisionally suggested, where the pre-exponential factor is based on that determined for the *i*-propyl group (see comment e). ^g Alk-1-enyl (vinyl) substituent is assumed to result in complete deactivation of OH addition to the aromatic ring, based on experimental and theoretical information reported for styrene (Bignozzi et al., 1981; Tuazon et al., 1993; Cho et al., 2014). ^h Based on optimization to data for phenol, 11 methyl-substituted phenols, catechol and 2 methyl-substituted catechols. Use of temperature dependent factors, $R_{\text{OH}}(o-) = R_{\text{OH}}(p-) = 0.69 \exp(395/T)$ and $R_{\text{OH}}(m-) = R_{\text{OH}}(ipso-) = 0.025 \exp(1360/T)$ allows for a reasonable representation of observed preferred temperature dependences for phenol and cresols. In the absence of data, the parameters are also assumed to apply to -OOH substituents. ⁱ Based on optimization to data for benzyl alcohol alone, with all factors assumed equivalent. In the absence of temperature dependence data, $R_{\text{C-OH}}(\Phi) = \exp(390/T)$ can be provisionally assumed in each case. ^j Strong deactivation of OH addition by -C(=O)H substituent optimized to recreate dominant (96 %) contribution of H abstraction from -C(=O)H substituent calculated by Iuga et al. (2008), with all factors assumed equivalent. Temperature dependence, $R_{\text{C(O)H}}(\Phi) = \exp(-698/T)$, is provisionally assumed in each case which (when combined with those for $F(\Phi)$ and k_{ipso}) results in a weak overall temperature dependence, consistent with calculations of Iuga et al. (2008). Factors also assumed to apply to -C(=O)R substituents. ^k Based on optimization to data for methoxybenzene and 1,2-dimethoxybenzene. Use of $R_{\text{OMe}}(o-) = R_{\text{OMe}}(p-) = \exp(365/T)$ and $R_{\text{OMe}}(m-) = R_{\text{OMe}}(ipso-) = \exp(-70/T)$ leads to overall weak negative temperature dependence near 298 K, consistent with data of Perry et al. (1977) over the range 300–320 K. Factors assumed to apply to -OR substituents in general (with the exception of -OPh groups), and are also assumed to apply to -OOR substituents in the absence of data. ^l Based on optimization to data for diphenyl ether alone, by scaling the optimized values of $R_{\text{OMe}}(\Phi)$. ^m Based on optimization to data for methyl salicylate alone, with all factors assumed equivalent. In the absence of temperature dependence data, $R_{\text{C(O)OMe}}(\Phi) = \exp(-400/T)$ can be provisionally assumed in each case. Factors assumed to apply to -C(=O)OR substituents in general. ⁿ Based on optimization to data for nitrobenzene, 1-methyl-3-nitrobenzene and four methyl-substituted 2-nitrophenols (with values of $R_{\text{OH}}(\Phi)$ applied, where appropriate). In the absence of temperature dependence data, $R_{\text{NO}_2}(o-) = R_{\text{NO}_2}(p-) = \exp(-1110/T)$ and $R_{\text{NO}_2}(m-) = R_{\text{NO}_2}(ipso-) = \exp(-792/T)$ can be provisionally assumed. Parameters are also assumed to apply to -ONO₂ substituents, in the absence of data.

DFT calculations of Alarcón et al. (2014) provide some support for this trend for $R_{i\text{-pr}}(o-)$. Provisional temperature dependences are also suggested for the other $R_{\text{alkyl}}(o-)$ and $R_{\text{alkyl}}(p-)$ values (see Table 6 comments), although it is again emphasized that these parameters are generally based on very limited information.

3.1.3 Alkenyl-substituted aromatic hydrocarbons

The set of preferred kinetic data contains rate coefficients for the reactions of OH with four alk-1-enyl (or vinyl) substituted aromatic hydrocarbons, namely styrene (ethenylbenzene), α -methylstyrene (*i*-propenylbenzene), β -methylstyrene (propenylbenzene) and β,β -dimethylstyrene (2-methylpropenylbenzene). Experimental and theoretical information for the most studied compound, styrene, is

consistent with the reaction occurring predominantly by addition of OH to the ethenyl substituent (Bignozzi et al., 1981; Tuazon et al., 1993; Cho et al., 2014). However, unlike the trends in rate coefficients for aliphatic alkenes (see Sect. 4.1.1 of Jenkin et al., 2018a), the presence of the alkyl substituents on the alkene group in the series of styrenes does not apparently enhance the reactivity, with very similar 298 K rate coefficients reported for styrene, α -methylstyrene and β -methylstyrene, and a reduction in reactivity for the most substituted compound, β,β -dimethylstyrene. A fixed rate coefficient, $k_{\text{C=C-Ph}} = 9.8 \times 10^{-12} \exp(530/T) \text{ cm}^3 \text{ molecule}^{-1} \text{ s}^{-1}$, is therefore provisionally assigned to addition of OH to alk-1-enyl (vinyl) substituents, based on the preferred value for styrene at 298 K, and the value of E/R calculated by Cho et al. (2014). The reaction is assumed to occur exclusively

by addition to the β carbon in the substituent group, because this forms a resonance-stabilized radical. Accordingly, the presence of an alk-1-enyl (vinyl) substituent is assumed to result in complete deactivation of OH addition to the aromatic ring (see Table 6).

The addition of OH to more remote C=C bonds in substituent groups in alkenyl-substituted aromatic hydrocarbons is expected to be well described by the methods described in the companion paper (Jenkin et al., 2018a), which update and extend the methods reported by Peeters et al. (2007) for alkenes and dienes. However, there are currently no data to test this assumption. In these cases, it is suggested that a default value of $R(\Phi) = 1.0$ for the remote alkenyl group is applied for addition of OH to the aromatic ring.

3.2 Monocyclic aromatic oxygenates

The preferred 298 K data include rate coefficients for reactions of OH with 42 aromatics containing a variety of oxygenated substituent groups, which were used to extend the methods described above for estimating rate coefficients for aromatic hydrocarbons. Rate coefficients for H-atom abstraction from the oxygenated groups are generally represented using the methods applied to aliphatic oxygenates (Jenkin et al., 2018a), in conjunction with the values of $F(X)$ given in Table 1, where appropriate; but with specific parameters defined for abstraction from -OH and -C(=O)H substituents (see Sect. 3.2.1–3.2.3). For addition of OH to the aromatic ring, the influences of the oxygenated substituents are described by the set of adjustment factors, $R(\Phi)$, given in Table 6. As for the higher alkyl substituents discussed in Sect. 3.1.2, these represent corrections to the values of $F(\Phi)$ in Table 3, and to k_{ipso} in Table 2, and are applied for each oxygenated substituent in the given molecule. They thus describe the effect of the oxygenated substituent relative to that of a -CH₃ group in the same position. In many cases, values of $R(\Phi)$ are derived from the analysis of a limited number of compounds containing the relevant substituent, with some based on reported data for a single compound, as summarized in the notes to Table 6. However, the values for -OH, -C(=O)H and -NO₂ are based on analysis of larger sets of compounds, as described in following subsections. With the exception of three catechols, the values of $R(\Phi)$ in Table 6 are determined from sets of compounds containing only one of the relevant oxygenated substituent. As a result, extrapolation of the method to compounds containing several activating substituents can result in unreasonably high estimated rate coefficients (i.e. exceeding the bimolecular collision rate). An upper-limit rate coefficient, $k_{\text{calc}} = 3.0 \times 10^{-10} \text{ cm}^3 \text{ molecule}^{-1} \text{ s}^{-1}$, is therefore imposed. Further data for aromatics containing multiple oxygenated substituents are clearly required to allow the method to be tested and refined.

3.2.1 Phenols and catechols

The contribution of H-atom abstraction from the -OH substituent in phenolic compounds has generally been inferred from the measured yields of nitrophenolic products, under conditions when the intermediate phenoxy radicals are expected to react predominantly with NO₂. Based on the nitrophenol yields reported for phenol and the set of cresol isomers by Atkinson et al. (1992), Olariu et al. (2002), Berndt and Böge (2003) and Coeur-Tourneur et al. (2006), an average rate coefficient, $k_{\text{abs(Ph-OH)}} = 2.6 \times 10^{-12} \text{ cm}^3 \text{ molecule}^{-1} \text{ s}^{-1}$, is assigned to this abstraction reaction at 298 K. This is about a factor of 20 greater than estimated for abstraction from -OH groups in aliphatic compounds (Jenkin et al., 2018a), which can be attributed to the resonance stabilization of the product phenoxy radicals. This suggests that the value of $k_{\text{abs(Ph-OH)}}$ may therefore be influenced by the presence of other substituents on the aromatic ring. This cannot be confirmed unambiguously from the reported dataset for phenols and cresols, although the presence of the *ortho* NO₂ group in 2-nitrophenols appears to have a significant deactivating effect (see Sect. 3.2.3). There is currently insufficient information to allow a full appraisal of the effects of the variety of possible substituent groups on H-atom abstraction from -OH (or other) substituents. In the present work, therefore, the above value of $k_{\text{abs(Ph-OH)}}$ is applied, unless the compound contains either an *ortho* NO₂ group or (by inference) a *para* NO₂ group. $k_{\text{abs(Ph-OH)}}$ is assumed to be independent of temperature over the atmospheric range, which is consistent with the provisional temperature dependence expressions suggested by Atkinson (1989), inferred from extrapolation of higher temperature data for phenol and *o*-cresol.

The values of $R_{\text{OH}}(\Phi)$ in Table 6 were varied iteratively to minimize the summed square deviation, $\Sigma((k_{\text{calc}} - k_{\text{obs}})/k_{\text{obs}})^2$ at 298 K for phenol, 14 methyl-substituted phenols, catechol and two methyl-substituted catechols. The resultant values of k_{calc} agree reasonably well with k_{obs} for the complete set of compounds (see Fig. 2), with particularly good agreement for the more substituted phenols and the catechols. Although the agreement is less good for the smaller, less reactive compounds (particularly for phenol, $k_{\text{calc}}/k_{\text{obs}} \approx 0.6$, and *p*-cresol, $k_{\text{calc}}/k_{\text{obs}} \approx 0.7$), the values of $R_{\text{OH}}(\Phi)$ are considered appropriate for wider application to multifunctional aromatic compounds containing -OH substituents for which there is currently no information. Temperature dependent data are currently limited to phenol and the cresol isomers. Use of the temperature dependent factors given in Table 6 allows for a reasonable representation of observed preferred temperature dependences, as shown in the inset of Fig. 2 (see also Fig. S2).

The attack distributions predicted by the optimized parameters recreate some of the features inferred from reported experimental studies for phenol and cresols (e.g. Olariu et al., 2002), initiating routes to the observed formation of cat-

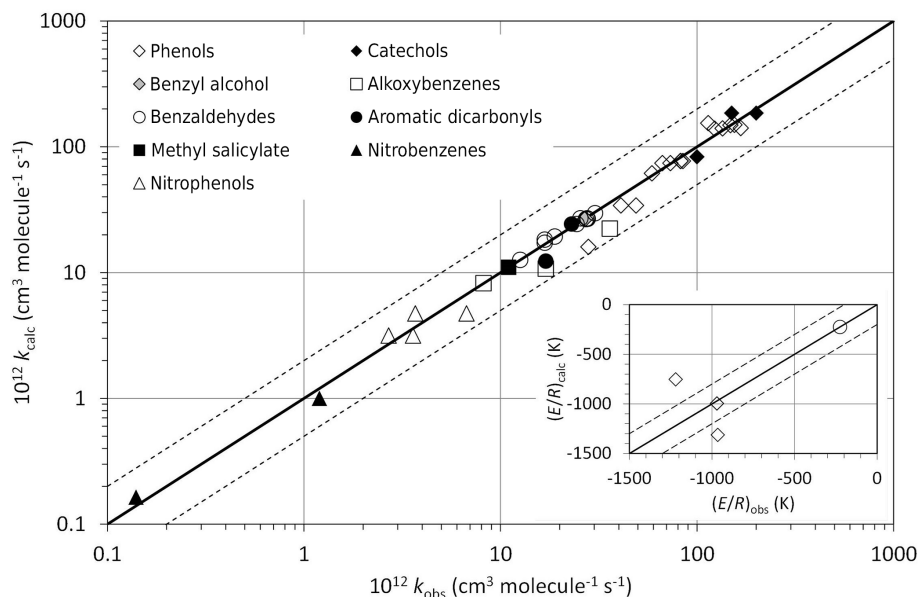


Figure 2. A log–log correlation of k_{calc} and k_{obs} at 298 K for oxygenated aromatic compounds. The broken lines show the factor of 2 range. The inset plot shows a correlation of the temperature coefficients $(E/R)_{\text{calc}}$ and $(E/R)_{\text{obs}}$ for phenol, cresols and benzaldehyde (note that the data points for *o*- and *p*-cresol are coincident at $(E/R)_{\text{obs}} = -970$ K, $(E/R)_{\text{calc}} = -996$ K). The broken lines show the ± 200 K range.

echols (1,2-dihydroxyarenes), benzoquinones and nitrophenols (see Sect. 4.2). As shown in Table 6, comparable values of $R_{\text{OH}}(\Phi)$ for each attack position are required to recreate the observed kinetics for the complete set of phenolic compounds. As a result, the -OH substituent retains the greater *ortho* and *para* directing influence discussed above for the reference substituent, -CH₃. The optimized parameters therefore predict significant formation of catechols from the oxidation of mono-phenols (resulting from *ortho* attack), qualitatively consistent with the results of the experimental studies. However, the optimized *ortho* directing influence of the -OH substituent is still insufficient to recreate the observed dominant (65–80 %) formation of catechol products, reported for phenols and cresols (e.g. Olariu et al., 2002). Noting that the product studies mainly consider the smaller compounds for which the parameter optimization procedure works least well, this may be indicative of the contribution of *ortho* attack of OH being underestimated for these compounds, but with the method being reasonable for wider application to more substituted aromatic products containing -OH substituents. It is generally recommended that attack distributions (and rate coefficients) based on the results of experimental studies are applied where evaluated information is available, as presented specifically for phenol and the cresol isomers in Sect. S3.

3.2.2 Benzaldehydes

The set of preferred kinetic data contains rate coefficients for benzaldehyde, three methyl-substituted benzaldehydes and six dimethyl-substituted benzaldehydes. In ad-

dition, preferred data are included for phthalaldehyde (1,2-diformylbenzene) and 2-acetylbenzaldehyde, and an upper-limit rate coefficient for the related compound 1,2-diacetylbenzene, based on Wang et al. (2006). The data show that the presence of methyl substituents in the benzaldehydes increases the OH reactivity systematically. It is generally accepted that abstraction of the H atom from the formyl (-C(=O)H) substituent is the dominant pathway for benzaldehyde, and this has been estimated to account for about 96 % of the reaction at 298 K in the DFT study of Iuga et al. (2008). As discussed previously (e.g. Thiault et al., 2002; Clifford et al., 2005; Clifford and Wenger, 2006), the activating effect of the methyl substituents may therefore result from an increasing contribution of OH addition and/or from an activating influence on the abstraction rate from the formyl substituent.

Initially, it was assumed that the rate coefficient for H-atom abstraction from the formyl group, $k_{\text{abs}}(\text{Ph-C(O)H})$, remains constant for the complete series of compounds. Values of $k_{\text{abs}}(\text{Ph-C(O)H})$, and of a set of adjustment factors for OH addition, $R_{\text{C(O)H}}(\Phi)$, were varied iteratively to minimize $\Sigma((k_{\text{calc}} - k_{\text{obs}})/k_{\text{obs}})^2$ at 298 K, leading to a set of parameter values given in Sect. S4 (Table S4 in the Supplement). These predict that the contribution of H-atom abstraction from benzaldehyde is 86 %, decreasing to 36–46 % for the dimethylbenzaldehyde isomers. Although this is consistent with a major contribution for benzaldehyde, the predicted value is significantly lower than the 96 % calculated for H-atom abstraction by Iuga et al. (2008). With the reasonable assumption that the values of $R_{\text{C(O)R}}(\Phi)$ for -C(=O)H substituents can also be applied more generally to -C(=O)R substituents, the

estimated rate coefficient for 1,2-diacetylbenzene also exceeds the reported upper-limit value by more than a factor of 2. This suggests that these optimized parameters also significantly overestimate OH addition to the aromatic ring.

An alternative procedure was therefore adopted in which the contribution of H-atom abstraction from the $-C(=O)H$ group in benzaldehyde was constrained to 96 % at 298 K (providing a reference value of $k_{\text{abs}}(\text{Ph}-C(O)H) = 1.21 \times 10^{-11} \text{ cm}^3 \text{ molecule}^{-1} \text{ s}^{-1}$); and the values of $R_{C(O)H}(\Phi)$ were varied to reproduce the total rate coefficient for benzaldehyde, leading to the (strongly deactivating) values presented in Table 6. The activating influence of the methyl substituents is then partly accounted for by increases in the OH addition rate coefficients, but also requires H-atom abstraction from the $-C(=O)H$ group to be enhanced. Based on optimization to the complete set of rate coefficients, the data were found to be well described by assigning activation factors of $\exp(115/T)$ (equating to a value of 1.47 at 298 K) for a methyl group positioned *ortho* to the $-C(=O)H$ group, and $\exp(78/T)$ (equating to a value of 1.30 at 298 K) for a methyl group positioned either *meta* or *para* to the $-C(=O)H$ group (with these factors also assumed to apply to other alkyl groups). A correlation of the optimized values of k_{calc} with k_{obs} at 298 K is shown in Fig. 2, with the estimation method reproducing all the observed values to within 10 %. Based on this approach, H-atom abstraction from the $-C(=O)H$ group remains the most important route, decreasing from 96 % for benzaldehyde to 76–88 % for the dimethylbenzaldehyde isomers. The optimized parameters also provide a reasonable description of the data for phthalaldehyde (1,2-diformylbenzene) and 2-acetylbenzaldehyde (identified as aromatic dicarbonyls in Fig. 2), and an estimated rate coefficient for 1,2-diacetylbenzene ($3.8 \times 10^{-13} \text{ cm}^3 \text{ molecule}^{-1} \text{ s}^{-1}$) that is consistent with the reported upper-limit value ($< 1.2 \times 10^{-12} \text{ cm}^3 \text{ molecule}^{-1} \text{ s}^{-1}$).

Temperature-dependent data are only available for benzaldehyde. Within the constraints of the approach described above, this was used to provide the optimized temperature dependence expression, $k_{\text{abs}}(\text{Ph}-C(O)H) = 5.23 \times 10^{-12} \exp(250/T) \text{ cm}^3 \text{ molecule}^{-1} \text{ s}^{-1}$.

3.2.3 Nitroarenes and nitrophenols

The set of preferred kinetic data contains rate coefficients for the reactions of OH with a number of nitro-substituted aromatics, namely nitrobenzene, 1-methyl-3-nitrobenzene, 2-nitrophenol and four methyl-substituted 2-nitrophenols. These data were used to optimize the values of $R_{\text{NO}_2}(\Phi)$ in Table 6, with the values of $R_{\text{OH}}(\Phi)$ determined in Sect. 3.2.1 applied where appropriate. During this procedure, it became clear that the value of $k_{\text{abs}}(\text{Ph}-OH)$ (also optimized in Sect. 3.2.1) substantially overestimates the importance of H-atom abstraction from the $-OH$ substituent in 2-nitrophenols. The data therefore suggest that an *ortho* NO_2 group (and pos-

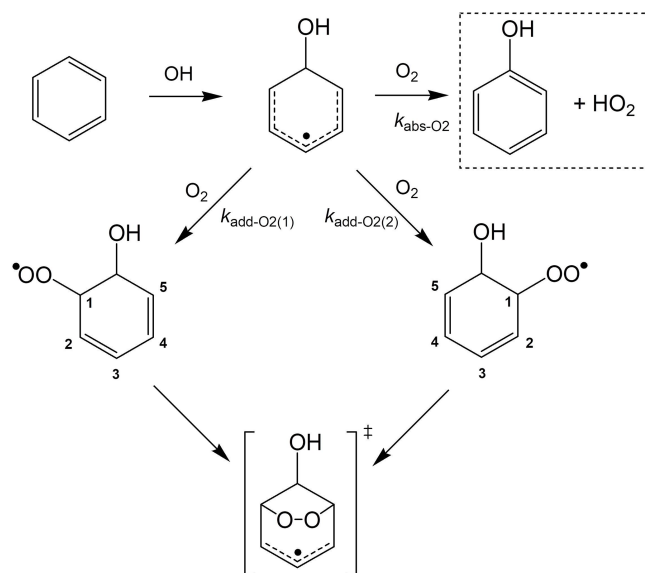


Figure 3. Schematic representation of the reaction of OH-aromatic adducts with O_2 , with alkyl substituents omitted for clarity. The abstraction pathway (for which the rate coefficient is $k_{\text{abs-O}_2}$) requires the presence of an α -H atom, and is therefore unavailable for adducts formed from OH addition *ipso* to an alkyl group. The rate coefficients for the two addition pathways ($k_{\text{add-O}_2(1)}$ and $k_{\text{add-O}_2(2)}$) depend on the number and distribution of alkyl substituents at positions 1 to 5 (see Sect. 4.1 and Table 8). The resultant β -hydroxy cyclohexadienylperoxy radicals are assumed to undergo prompt ring closure to produce a common “peroxide-bicyclic” radical.

sibly also a *para* NO_2 group) has a strong deactivating effect on this reaction, and the data were best described by reducing its rate by at least an order of magnitude, compared with $k_{\text{abs}}(\text{Ph}-OH)$. It was therefore assumed that the rate coefficient previously assigned to $-OH$ groups in aliphatic compounds, $k_{\text{abs}}(-OH) = 1.28 \times 10^{-12} \exp(-660/T) \text{ cm}^3 \text{ molecule}^{-1} \text{ s}^{-1}$, applies when the aromatic ring is deactivated by the presence of an NO_2 group *ortho* or *para* to the $-OH$ substituent. As indicated above, additional information is clearly required to allow a full appraisal of the effects of substituent groups on H-atom abstraction from $-OH$ (or other) substituents in aromatic compounds.

The optimized values of $R_{\text{NO}_2}(\Phi)$ in Table 6 indicate that NO_2 substituents also strongly deactivate addition of OH to the aromatic ring. As shown in Fig. 2, the resultant values of k_{calc} agree well with k_{obs} for the complete set of nitro-substituted compounds identified above.

Table 7. Partial rate coefficients for the reactions of O₂ with OH-aromatic adducts, and their temperature dependences described by $k = A \exp(-(E/R)/T)$. Parameters are shown for abstraction of hydrogen α to the -OH group ($k_{\text{abs-O}_2}$) and the reference rate coefficient for β O₂ addition adjacent to the -OH substitution ($k_{\text{add-O}_2}^\circ$).

Parameter	A (10^{-14} cm ³ molecule ⁻¹ s ⁻¹)	E/R (K)	$k_{298\text{ K}}$ (10^{-17} cm ³ molecule ⁻¹ s ⁻¹)	Comment
$k_{\text{abs-O}_2}$	1.75	1500	11.4	a,b
$k_{\text{add-O}_2}^\circ$	1.50	1700	5.0	b,c

Comments: ^a value of E/R based on the activation energy calculated for H atom abstraction from the OH-benzene adduct by Raoult et al. (2004). ^b Value of A for k_{abs} and of k_{add}° at 298 K optimized so that $k_{\text{abs}} + 2k_{\text{add}}^\circ \approx 2.1 \times 10^{-16}$ cm³ molecule⁻¹ s⁻¹, and $k_{\text{abs}}/(k_{\text{abs}} + 2k_{\text{add}}^\circ) \approx 0.53$ at 298 K, consistent with IUPAC recommendations (IUPAC, 2017b) and the literature. ^c Value of A for k_{add}° set to be consistent with calculations of Raoult et al. (2004), with E/R automatically returned from A and the 298 K value of k_{add}° .

4 Reaction of O₂ with OH-aromatic adducts and subsequent chemistry

4.1 OH-aromatic hydrocarbon adducts

A method has been developed to describe the chemistry initiated by reaction of O₂ with the OH-aromatic adducts formed from the addition of OH radicals to aromatic hydrocarbons. Theoretical studies have shown that these reactions, and the subsequent reaction sequences, can be highly complex, involving the participation of geometrical isomers of very different reactivities (e.g. Raoult et al., 2004; Glowacki et al., 2009; Wu et al., 2014; Li et al., 2014; Pan and Wang, 2014; Vereecken, 2018a). The present method does not include the level of detail established in these studies, but aims to provide an empirically optimized reaction framework incorporating the main features of the mechanisms, as reported in both laboratory and theoretical work.

The reactions of the OH-aromatic hydrocarbon adducts with O₂ are represented to react either by direct α -H-atom abstraction, forming HO₂ and an hydroxyarene (phenolic) product, or by β -O₂ addition to the aromatic ring at each of the two carbon atoms adjacent to the -OH substituent to produce β -hydroxy cyclohexadienylperoxy radicals (as illustrated in Fig. 3), such that the overall rate coefficient is given by $k_{\text{abs-O}_2} + k_{\text{add-O}_2(1)} + k_{\text{add-O}_2(2)}$. The H-atom abstraction reaction is unavailable for adducts formed from OH addition *ipso* to an alkyl substitution. There is some evidence for a “dealkylation” pathway from such adducts (e.g. Noda et al., 2009), but this is not currently represented owing to conflicting evidence on its significance (e.g. Aschmann et al., 2010; Loison et al., 2012). In practice, the β -O₂ addition pathways are reversible, such that each value of $k_{\text{add-O}_2}$ specifically quantifies the effective irreversible component of the reaction that results in onward removal of the given cyclohexadienylperoxy radical (IUPAC, 2017b, c).

The value of $k_{\text{abs-O}_2}$ and the reference value of $k_{\text{add-O}_2}^\circ$ for the benzene system (see Table 7) are informed by the calculations of Raoult et al. (2004), but adjusted to give a total rate coefficient of $\sim 2.1 \times 10^{-16}$ cm³ molecule⁻¹ s⁻¹ at 298 K for (the irreversible component of) the reaction of HOC₆H₆ with

Table 8. Substituent factors $F_i(X)$ for the addition of O₂ to aromatic adducts reactions of OH to aromatic hydrocarbons, and their temperature dependences described by $F_i(X) = \exp(-B_{F_i(X)}/T)$ ^a.

Location of substituent ^b	Parameter	$B_{F_i(X)}$	$F_i(X)_{298\text{ K}}$
1	$F_1(-\text{alkyl})$	0	1.0
2	$F_2(-\text{alkyl})$	−207	2.0
3	$F_3(-\text{alkyl})$	−620	8.0
4	$F_4(-\text{alkyl})$	−207	2.0
5	$F_5(-\text{alkyl})$	−558	6.5

Comments: ^a values of $F_i(X)_{298\text{ K}}$ optimized to recreate the trend in yields of hydroxyarene (phenolic) products for toluene, *m*-xylene, *p*-xylene, 1,2,4-trimethylbenzene and 1,3,5-trimethylbenzene (see Table 3). The values are therefore based on data for methyl substituents, but are assumed to apply to alkyl substituents in general. Values of $B_{F_i(X)}$ assume that the temperature dependence of $F_i(X)$ can be described by $\exp(-B_{F_i(X)}/T)$. ^b As shown in Fig. 3 and discussed in Sect. 4.1.

O₂, as recommended by IUPAC (2017b); and a yield of phenol of $\sim 53\%$, which is also consistent with the literature. The value of $k_{\text{abs-O}_2}$ is assumed to be independent of the presence of alkyl substituents, but the value of $k_{\text{add-O}_2}$ depends on both the degree and distribution of alkyl substituents, and is given by

$$k_{\text{add-O}_2} = k_{\text{add-O}_2}^\circ \prod F_i(X), \text{ for } n = 0(\text{or } 1) \quad (6)$$

$$k_{\text{add-O}_2} = k_{\text{add-O}_2}^\circ \prod F_i(X)/n^{0.5}, \text{ for } n \geq 1 \quad (7)$$

Here, n is the number of alkyl substituents (in positions 1 to 5 relative to the addition of O₂), and $F_i(X)$ is the activating effect of each alkyl substituent in terms of its position (see Fig. 3). The assigned values of $F_i(X)$ (given in Table 8) recreate the reported general trend in total hydroxyarene yields for methyl-substituted aromatics, and also a reasonable representation of the reported distribution of isomers formed from a given aromatic precursor (see Table S1). In the case of the toluene system, for example, the optimized parameters provide respective yields of 12.2, 3.7 and 3.3 % for *o*-, *m*- and *p*-cresol, and a total rate coefficient of 5.7×10^{-16} cm³ molecule⁻¹ s⁻¹ for the reaction of

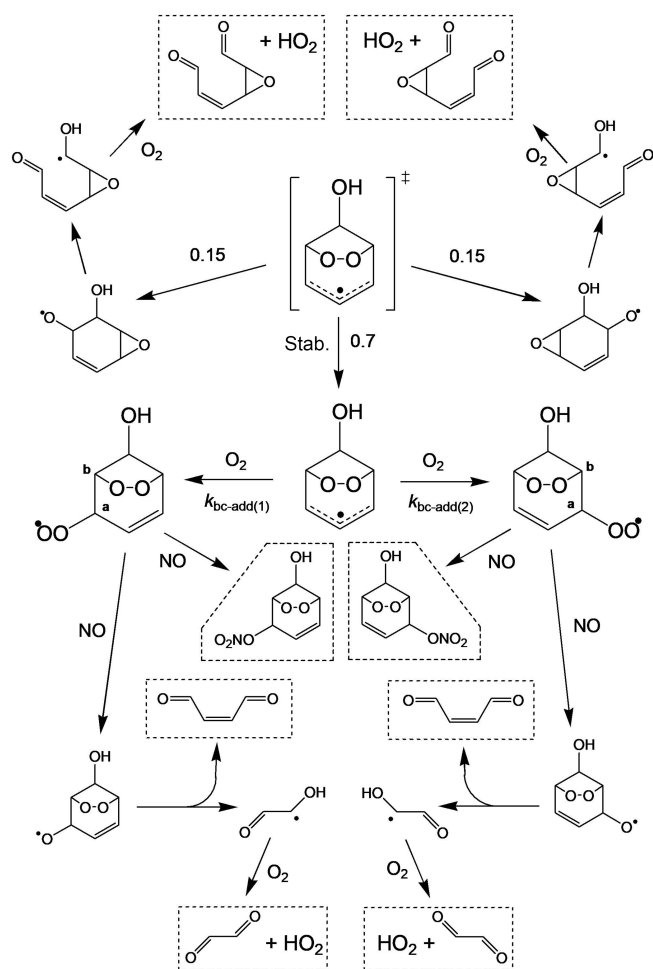


Figure 4. Schematic representation of the mechanism following formation of the “peroxide-bicyclic” radical, as shown in Fig. 3, with alkyl substituents omitted for clarity. The initial energy-rich “peroxide-bicyclic” radical is represented to isomerize as shown with a total optimized probability of 30 % in competition with stabilization (see Sect. 4.1). Addition of O_2 to the stabilized radical can occur at two positions. The rate coefficients for the two addition pathways ($k_{\text{bc-add}(1)}$ and $k_{\text{bc-add}(2)}$) depend on the number and distribution of alkyl substituents at positions “a” and “b” in each case (see Sect. 4.1 and Table 9). The resultant peroxy radicals undergo conventional bimolecular reactions, with only those involving NO shown here. The oxy radicals formed from propagating channels decompose to form α -dicarbonyls and (at least partially) unsaturated 1,4-dicarbonyl products, in conjunction with HO_2 , via the generally accepted mechanism shown.

O_2 with the set of OH-toluene adducts (i.e. HOC_7H_8) at 298 K; in very good agreement with the IUPAC recommendations (IUPAC, 2017c). To a first approximation, the simpler expression in Eq. (6) provides an acceptable description for the complete series of aromatics, but leads to a systematic underestimation of the hydroxyarene yields reported for *m*-xylene, *p*-xylene, 1,2,4-trimethylbenzene and 1,3,5-trimethylbenzene. The adjusted expression in Eq. (7) is there-

Table 9. Substituent factors, $F_a(\text{X})$ and $F_b(\text{X})$, for addition of O_2 to stabilized peroxide-bicyclic radicals. Parameters shown are for 298 K, but are assumed to apply to the atmospheric temperature range^a.

Substituent	$F_a(\text{X})$	$F_b(\text{X})$	Comment
-H	1	1	–
alkyl	1000	3	b, c
oxygenated substituents	see comment		d

Comments: ^a factors related to addition of O_2 at positions “a” and “b” in Fig. 4 as discussed in Sect. 4.1. ^b Activating effects of alkyl substituents are informed by calculations for structures formed in the toluene system by Wu et al. (2014) and in the 1,2,4-trimethylbenzene system Li et al. (2014), with a particularly strong effect for substitution at position “a”. The assigned values were optimized to allow a reasonable representation of the relative yields of α -dicarbonyl products from methyl-substituted aromatics (see Sect. 4.1, Fig. 5 and Table S2). The values are therefore based on data for methyl substituents, but are assumed to apply to alkyl substituents in general. ^c Also applied to substituted alkyl groups not covered by comment d. ^d If the resonant peroxide-bicyclic radical contains an oxygenated substituent at either or both positions “a”, addition of O_2 is assumed to occur at the site possessing the substituent that is higher in the list given in Sect. 4.2.

fore defined to allow a more precise description of the reported hydroxyarene yields for the more substituted species.

As shown in Fig. 3, the two β -hydroxy cyclohexadienylperoxy radicals formed from O_2 addition are represented to undergo prompt ring closure to produce a common hydroxy-dioxa-bicyclo or “peroxide-bicyclic” radical. This process has been reported to dominate over alternative bimolecular reactions of the peroxy radicals under atmospheric conditions (e.g. Suh et al., 2003; Raoult et al., 2004; Glowacki et al., 2009; Wu et al., 2014; Li et al., 2014; Pan and Wang, 2014). The subsequent chemistry of the peroxide-bicyclic radical is shown in Fig. 4. In each case, the energy-rich radical either promptly isomerizes to form two cyclic epoxy-oxy radicals (as originally proposed by Bartolotti and Edney, 1995), or is stabilized and adds O_2 to form two possible peroxide-bridged peroxy radicals. The cyclic epoxy-oxy radicals undergo ring-opening, followed by reaction with O_2 to generate HO_2 and an epoxydicarbonylene product in each case. Evidence for the formation of the epoxydicarbonylene products has been reported in experimental studies of a number of atmospheric systems (e.g. Yu and Jeffries, 1997; Kwok et al., 1997; Baltaretu et al., 2009; Birdsall et al., 2010; Birdsall and Elrod, 2011), although it is noted that their formation is calculated to be more important at reduced pressures (e.g. Glowacki et al., 2009; Li et al., 2014). In the present method, prompt isomerization of the peroxide-bicyclic radical to the cyclic epoxy-oxy radicals is assigned a total structure-independent branching ratio of 0.3, divided equally between the two available routes. As indicated above, the subsequent chemistry leads to prompt formation of HO_2 (i.e. not delayed by first requiring conversion of an organic peroxy radical to an oxy radical via a bimolecular reaction), which supplements that formed in conjunction with the hydroxyarene (phenolic) products (see Fig. 3). Inclusion of the

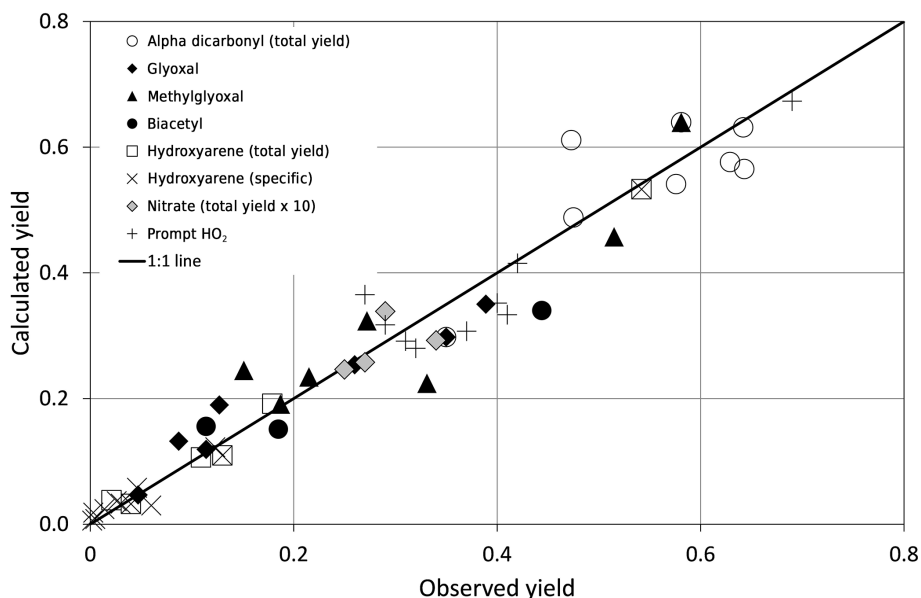


Figure 5. Correlation of calculated and observed yields of hydroxyarenes (total and specific), α -dicarbonyls (total and specific), peroxide-bicyclic nitrates (total) and prompt HO_2 formed from the degradation of benzene and methyl-substituted aromatic hydrocarbons. Observed data taken from Atkinson and Aschmann (1994), Smith et al. (1998, 1999), Klotz et al. (1998), Volkamer et al. (2001, 2002), Berndt and Böge (2006), Noda et al. (2009), Rickard et al. (2010), Elrod (2011) and Nehr et al. (2011, 2012), as summarized in Tables S1 and S2.

“epoxy-oxy” route with this optimized branching ratio results in total prompt HO_2 yields which provide a good representation of those reported by Nehr et al. (2011, 2012), and also total yields of the well established α -dicarbonyl products (formed from the alternative O_2 addition chemistry) that are consistent with those reported (see below). However, it is noted that this is an area of significant uncertainty, with theoretical studies predicting a much lower importance of the “epoxy-oxy” route at atmospheric pressure than applied here (e.g. Vereecken, 2018a, b; and references therein). Further studies are required to elucidate the sources of epoxydicarbonylenes and prompt HO_2 in aromatic systems.

The (stabilized) peroxide-bicyclic radical possesses an allyl resonance, such that addition of O_2 can occur at two possible positions, as shown in Fig. 4. The overall rate coefficient is therefore given by $k_{\text{bc-add}(1)} + k_{\text{bc-add}(2)}$. The reference rate coefficient, $k_{\text{bc-add}}^\circ$, for a system with no alkyl substituents at either positions “a” or “b” (see Table 9) was assigned a value of $4 \times 10^{-16} \text{ cm}^3 \text{ molecule}^{-1} \text{ s}^{-1}$, based on the total rate coefficient calculated for the peroxide-bicyclic radical formed in the benzene system by Glowacki et al. (2009). Reported calculations for methyl-substituted aromatics (e.g. Wu et al., 2014; Li et al., 2014) suggest that the value of $k_{\text{bc-add}}$ for a given system is also potentially influenced by the presence of alkyl substituents in positions “a” or “b”. The addition rate coefficient estimated here is therefore given by

$$k_{\text{bc-add}} = k_{\text{bc-add}}^\circ F_a(X) F_b(X). \quad (8)$$

Here, $F_a(X)$ and $F_b(X)$ quantify the activating effect of substituents in positions “a” and “b”, respectively. The as-

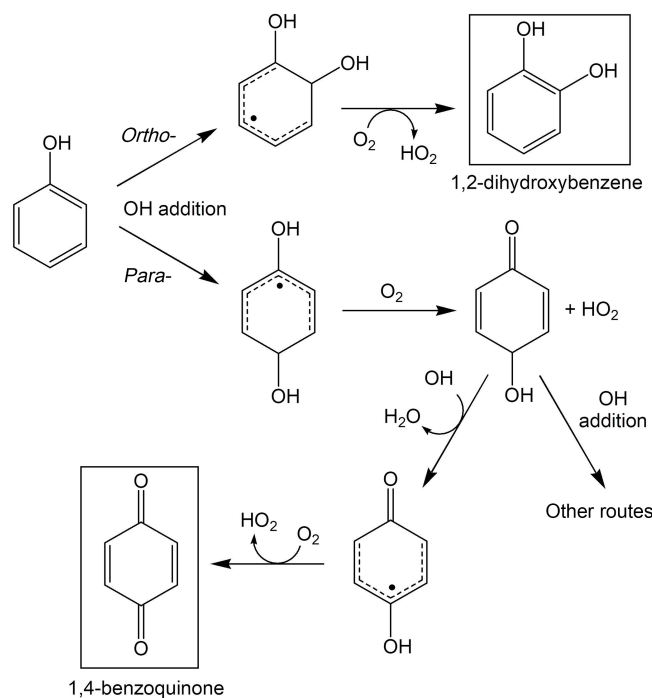


Figure 6. Routes applied following OH addition at an unsubstituted carbon *ortho* or *para* to an existing OH substituent in hydroxy-substituted aromatic compounds, using phenol as an example (see Sect. 4.2).

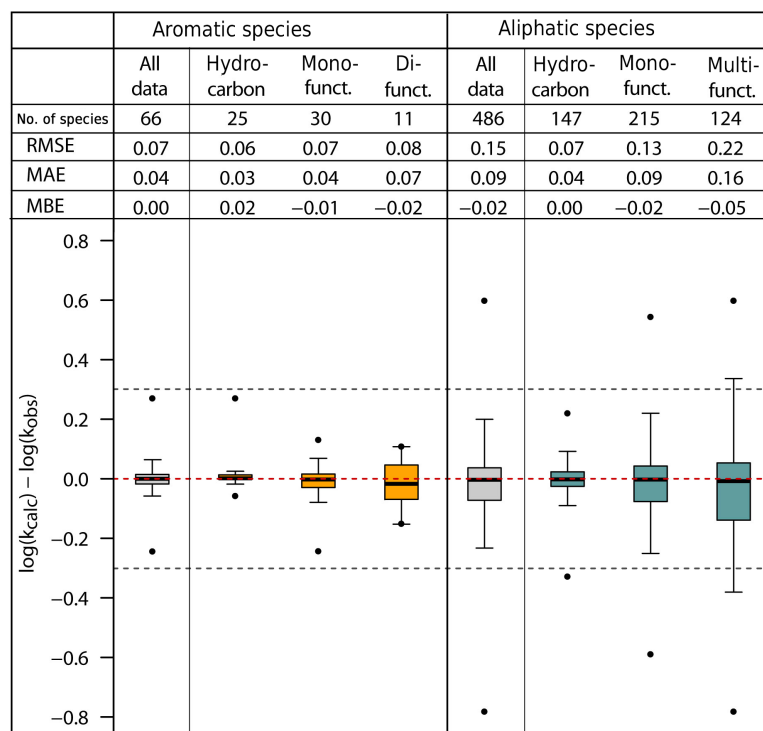


Figure 7. Root mean square error (RMSE), mean absolute error (MAE), mean bias error (MBE) and box plot for the error distribution in the estimated $\log k_{298\text{ K}}$ values for the full set and subsets of the aromatic species in the database, and for the aliphatic species reported previously (Jenkin et al., 2018a). The bottom and the top of the boxes are the 25th (Q_1) and 75th percentiles (Q_3), the black band is the median value. The whiskers extend to the most extreme data points which is no more than $1.5 \times (Q_3 - Q_1)$ from the box. The points are the extrema of the distribution. The black dotted lines correspond to agreement within a factor 2.

signed values for an alkyl substituent (given in Table 9) allow a reasonable representation of the relative distribution of α -dicarbonyl products (i.e. glyoxal, methylglyoxal and biacetyl) reported for the series of methyl-substituted aromatics for conditions when the peroxy radicals react predominantly with NO (see Table S2). The large value of $F_a(-\text{alkyl})$ indicates that addition of O_2 at an alkyl-substituted site in the resonant radical is strongly favoured, and can be assumed to be exclusive if only one of the two possible addition sites is alkyl substituted. The more modest influence of a substituent at position “b” (characterized by $F_b(-\text{alkyl})$) also influences the relative formation of the specific α -dicarbonyls (and their co-products) in cases where neither or both radical sites possess alkyl substituents. It is noted that the treatment of these structurally complex allyl radicals differs from that reported in the companion paper (Jenkin et al., 2018a) for generic allyl radicals, and is specific to this type of structure.

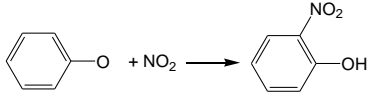

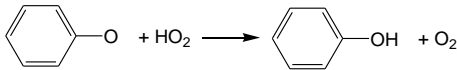
The calculated yields presented in Table S2 also take account of minor formation of nitrate products from the peroxy + NO reactions (see Fig. 4), for which the currently estimated branching ratios vary from 0 to 0.11 depending on peroxy radical structure. This is described in more detail elsewhere (Jenkin et al., 2018b). Table S2 also compares the calculated “prompt” yields of HO_2 with those reported by Nehr

et al. (2011, 2012) and the total nitrate yields with those reported by Rickard et al. (2010) and Elrod (2011). Figure 5 presents a correlation plot of calculated and observed yields of hydroxyarenes (total and specific), α -dicarbonyls (total and specific), nitrates (total) and prompt HO_2 , which confirms that the methods presented above provide a reasonable representation of the first-generation OH-initiated chemistry of aromatic hydrocarbons. Section S6 provides example calculations for the methods described above for the chemistry initiated by reaction of O_2 with the OH-aromatic adducts formed from the addition of OH to toluene.

4.2 OH-aromatic oxygenate adducts

Product and mechanistic information on the reactions of adducts formed from the addition of OH radicals to aromatic oxygenates appears to be limited to those formed from hydroxyarene (phenolic) compounds (e.g. Olariu et al., 2002; Berndt et al., 2003; Coeur-Tourneur et al., 2006). Those studies have established that 1,2-dihydroxyarenes (catechols) and 1,4-benzoquinones are formed as ring-retaining products of the OH-initiated oxidation of phenol and cresols. On the basis of the reported information, the pathways presented in Fig. 6 are applied in relation to hydroxy-substituted aromatic compounds. Addition of OH at an unsubstituted carbon *ortho*

Table 10. Reactions represented for phenoxy and substituted phenoxy radicals, and their assigned rate coefficients (in units $\text{cm}^3 \text{ molecule}^{-1} \text{ s}^{-1}$).

Reaction	Rate coefficient	Comment
	1.0×10^{-12}	^a
	2.9×10^{-13}	^b
	2.3×10^{-13}	^c

Comments: ^a rate coefficient per unsubstituted *ortho* site, based on that reported for $\text{C}_6\text{H}_5\text{O}$ by Platz et al. (1998), and assumed to apply over the tropospheric temperature range. ^b Rate coefficient based on that reported for $\text{C}_6\text{H}_5\text{O}$ by Tao and Li (1999), and assumed to apply over the tropospheric temperature range. The products of the reaction were not characterized and are assumed here. ^c Represented on the basis of evidence reported by Jenkin et al. (2007, 2010) and Herbinet et al. (2013) (see Sect. 5). In the absence of kinetics determinations, the rate coefficient is assumed equal to that calculated for the reaction $\text{CH}_3\text{O} + \text{HO}_2 \rightarrow \text{CH}_3\text{OH} + \text{O}_2$ by Mousavipour and Homayoon (2011), which is reported to be insensitive to temperature over the range 300–3000 K.

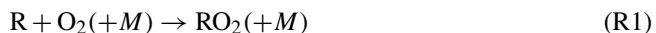
to an existing hydroxy substituent is assumed to result in exclusive formation of HO_2 and a 1,2-dihydroxy product, following subsequent reaction of the adduct with O_2 . Addition of OH *para* to an existing hydroxy substituent is assumed to result in the formation of HO_2 and a reactive 4-hydroxy-cyclohexa-2,5-dienone product, following subsequent reaction of the adduct with O_2 . In cases where the initial addition of OH occurs at an unsubstituted carbon in the aromatic compound, further reaction of OH with the 4-hydroxy-cyclohexa-2,5-dienone partially produces a 1,4-benzoquinone product (as shown in Fig. 6), based on the methods applied to aliphatic compounds (Jenkin et al., 2018a).

For other OH-aromatic oxygenate adducts, the mechanisms applied to OH-aromatic hydrocarbon adducts (see Sect. 4.1) are provisionally applied, in the absence of information. Within the framework described in Sect. 4.1, some additional assumptions are applied in relation to addition of O_2 to the (stabilized) resonant peroxide-bicyclic radical, these being consistent with those applied generally to allyl radicals containing oxygenated substituents (Jenkin et al., 2018a). If the resonant peroxide-bicyclic radical contains an oxygenated substituent at either or both positions “a”, addition of O_2 is assumed to occur exclusively at the site possessing the substituent that is higher in the following list:

$-\text{OH}/-\text{OR}/-\text{OOH}/-\text{OOR} > -\text{OC}(=\text{O})\text{H}/-\text{OC}(=\text{O})\text{R} > \text{alkyl}/-\text{H} > -\text{C}(=\text{O})\text{H}/-\text{C}(=\text{O})\text{R} > -\text{C}(=\text{O})\text{OH}/-\text{C}(=\text{O})\text{OR} > -\text{ONO}_2 > -\text{NO}_2$ (substituents with more remote oxygenated groups are treated as alkyl groups). If both sites possess a substituent of the same rating, O_2 addition is assumed to occur equally at each site. An oxygenated substituent at position “b” is assumed to have no effect (Table 9).

5 Reactions of organic radicals formed from OH attack on substituent groups

Carbon-centred organic radicals (R) formed from H-atom abstraction from, or OH addition to, substituent groups in aromatic compounds generally react as described for those formed from aliphatic organic compounds in the companion paper (Jenkin et al., 2018a). In the majority of cases, therefore, they react rapidly and exclusively with molecular oxygen (O_2) under tropospheric conditions to form the corresponding thermalized peroxy radicals (RO_2), the chemistry of which will be summarized elsewhere (Jenkin et al., 2018b):



(*M* denotes a third body, most commonly N_2 .) Abstraction of hydrogen from hydroxy and hydroperoxy substituent groups in aromatic VOCs results in the formation of phenoxy and phenyl peroxy radicals, respectively. The representation of phenyl peroxy radical chemistry will be considered elsewhere, along with that of other peroxy radicals (Jenkin et al., 2018b). The chemistry of phenoxy radicals differs from that of oxy radicals in general, in that they apparently do not react with O_2 , isomerize or decompose under tropospheric conditions. Kinetic studies for the phenoxy radical itself ($\text{C}_6\text{H}_5\text{O}$) indicate that reactions with NO, NO_2 and O_3 are likely to be competitive under ambient conditions (Platz et al., 1998; Berho et al., 1998; Tao and Li, 1999), with evidence also reported for reaction with HO_2 at room temperature (Jenkin et al., 2007, 2010) and in low-temperature combustion systems (Herbinet et al., 2013). As summarized in Table 10, the reactions with NO_2 , O_3 and HO_2 are generally represented for a given phenoxy radical, although reaction with NO_2 is unavailable for phenoxy radicals with two *ortho* substituents, because formation of a 1-hydroxy-2-nitroarene product is

precluded. The reaction with NO is not represented because the reverse reaction is reported to occur on the timescale of about 1 min (Berho et al., 1998).

6 Conclusions

A structure activity relationship (SAR) method has been developed to estimate rate coefficients for the reactions of the OH radical with aromatic organic species. This group contribution method was optimized using a database including a set preferred rate coefficients for 67 species. The overall performance of the SAR in determining $\log k_{298\text{K}}$ is now summarized.

The distribution of errors ($\log k_{\text{calc}}/k_{\text{obs}}$), the root mean squared error (RMSE), the mean absolute error (MAE) and the mean bias error (MBE) were examined to assess the overall reliability of the SAR. The RMSE, MAE and MBE are here defined as:

$$\text{RMSE} = \sqrt{\frac{1}{n} \sum_{i=1}^n (\log k_{\text{calc}} - \log k_{\text{obs}})^2}, \quad (9)$$

$$\text{MAE} = \frac{1}{n} \sum_{i=1}^n |\log k_{\text{calc}} - \log k_{\text{obs}}|, \quad (10)$$

$$\text{MBE} = \frac{1}{n} \sum_{i=1}^n (\log k_{\text{calc}} - \log k_{\text{obs}}), \quad (11)$$

where n is the number of species in the dataset. The assessment was performed to identify possible biases within a series of categories, namely hydrocarbons, monofunctional oxygenated species and bifunctional oxygenated species. Errors computed for these subsets are summarized in Fig. 7, where they are compared with those for the corresponding categories of aliphatic organic compounds, as reported in the companion paper (Jenkin et al., 2018a).

The calculated $\log k_{298\text{K}}$ shows no significant bias, with MBE remaining below 0.02 log units for the various subsets, and with median values of the error distributions close to zero. The reliability of the SAR decreases with the number of oxygenated functional groups on the aromatic ring, with the RMSE increasing from 0.06 for hydrocarbons to 0.07 for monofunctional and 0.08 for bifunctional species, i.e. a relative error for the calculated $k_{298\text{K}}$ of a 15, 17 and 20 %, respectively. This shows a similar pattern to that reported previously for the much larger dataset of aliphatic species (Jenkin et al., 2018a), but with systematically lower errors. As described in Sect. 3.2, some of the classes of aromatic oxygenated species contain data for only a single compound, such that the optimized parameters inevitably provide a good description of the observed data, whereas the aliphatic data are typically comprised of larger and more diverse sets of species. Additional rate coefficients would therefore be highly valuable for further assessment and evaluation of the SAR for a variety of aromatic oxygenated species. Finally,

for the full database, the SAR gives generally reliable $k_{298\text{K}}$ estimates, with a MAE of 0.04 and a RMSE of 0.07, corresponding to an overall agreement of the calculated $k_{298\text{K}}$ within 17 %.

Data availability. All relevant data and supporting information have been provided in the Supplement.

The Supplement related to this article is available online at <https://doi.org/10.5194/acp-18-9329-2018-supplement>.

Author contributions. All authors defined the scope of the work. MEJ developed the SAR methods and drafted the manuscript, which were both reviewed by all co-authors. RV and BA tested the SAR methods in GECKO-A and carried out the statistical analysis in Sect. 6.

Competing interests. The authors declare that they have no conflict of interest.

Acknowledgements. This work received funding from the Alliance of Automobile Manufacturers, and as part of the MAGNIFY project, with funding from the French National Research Agency (ANR) under project ANR-14-CE01-0010, and the UK Natural Environment Research Council (NERC) via grant NE/M013448/1. It was also partially funded by the UK National Centre for Atmospheric Sciences (NCAS) Composition Directorate. Marie Camredon (LISA, Paris) and Mike Newland (University of York) are gratefully acknowledged for helpful discussions on this work. We also thank Luc Vereecken (Forschungszentrum Jülich) for providing detailed comments during the open discussion, and two anonymous referees for review comments, that helped to improve the manuscript.

Edited by: Andreas Hofzumahaus

Reviewed by: two anonymous referees

References

- Alarcón, P., Bohn, B., Zetzsch, C., Rayez, M.-T., and Rayez, J.-C.: Reversible addition of the OH radical to *p*-cymene in the gas phase: multiple adduct formation. Part 2, Phys. Chem. Chem. Phys., 16, 17315–17326, 2014.
- Andreae, M. O. and Crutzen, P. J.: Atmospheric aerosols: biogeochemical sources and role in atmospheric chemistry, Science, 276, 1052–1058, 1997.
- Aschmann, S. M., Arey, J., and Atkinson, R.: Extent of H-atom abstraction from OH + *p*-cymene and upper limits to the formation of cresols from OH + *m*-xylene and OH + *p*-cymene, Atmos. Environ., 44, 3970–3975, 2010.

- Aschmann, S. M., Arey, J., and Atkinson, R.: Formation of *p*-cymene from OH + γ -terpinene: H-atom abstraction from the cyclohexadiene ring structure, *Atmos. Environ.*, 45, 4408–4411, 2011.
- Aschmann, S. M., Arey, J., and Atkinson, R.: Rate constants for the reactions of OH radicals with 1,2,4,5-tetramethylbenzene, pentamethylbenzene, 2,4,5-trimethylbenzaldehyde, 2,4,5-trimethylphenol, and 3-methyl-3-hexene-2,5-dione and products of OH + 1,2,4,5-tetramethylbenzene, *J. Phys. Chem. A*, 117, 2556–2568, 2013.
- Atkinson, R.: A structure-activity relationship for the estimation of rate constants for the gas-phase reactions of OH radicals with organic compounds, *Int. J. Chem. Kinet.*, 19, 799–828, 1987.
- Atkinson, R.: Kinetics and mechanisms of the gas-phase reactions of the hydroxyl radical with organic compounds, *J. Phys. Chem. Ref. Data*, Monograph 1, 246 pp., 1989.
- Atkinson, R. and Arey, J.: Atmospheric degradation of volatile organic compounds, *Chem. Rev.*, 103, 4605–4638, 2003.
- Atkinson, R. and Aschmann, S. M.: Products of the gas-phase reactions of aromatic hydrocarbons: Effect of NO₂ concentration, *Int. J. Chem. Kinet.*, 26, 929–944, 1994.
- Atkinson, R., Aschmann, S. M., and Arey, J.: Reactions of OH and NO₃ radicals with phenol, cresols, and 2-nitrophenol at 296 ± 2 K, *Environ. Sci. Technol.*, 26, 1397–1403, 1992.
- Aumont, B., Szopa, S., and Madronich, S.: Modelling the evolution of organic carbon during its gas-phase tropospheric oxidation: development of an explicit model based on a self generating approach, *Atmos. Chem. Phys.*, 5, 2497–2517, <https://doi.org/10.5194/acp-5-2497-2005>, 2005.
- Baltaretu, C. O., Lichtman, E. I., Hadler, A. B., and Elrod, M. J.: Primary atmospheric oxidation mechanism for toluene, *J. Phys. Chem. A*, 113, 221–230, 2009.
- Bartolotti, L. J. and Edney, E. O.: Density functional theory derived intermediates from the OH initiated atmospheric oxidation of toluene, *Chem. Phys. Lett.*, 245, 119–122, 1995.
- Bedjanian, Y., Morin, J., and Romanias, M. N.: Gas-phase reaction of hydroxyl radical with *p*-cymene over an extended temperature range, *J. Phys. Chem. A*, 119, 11076–11083, <https://doi.org/10.1021/acs.jpca.5b08478>, 2015.
- Berho, F. and Lesclaux, R.: Berho, F., Caralp, F., Rayez, M. T., Lesclaux, R., and Ratajczak, E.: Kinetics and thermochemistry of the reversible combination reaction of the phenoxy radical with NO, *J. Phys. Chem. A*, 102, 1–8, 1998.
- Bernard, F., Magneron, I., Eyglunent, G., Dale, V., and Wallington, T. J.: Atmospheric chemistry of benzyl alcohol: kinetics and mechanism of reaction with OH radicals, *Environ. Sci. Technol.*, 47, 3182–3189, 2013.
- Berndt, T. and Böge, O.: Gas-phase reaction of OH radicals with phenol, *Phys. Chem. Chem. Phys.*, 5, 342–350, 2003.
- Berndt, T. and Böge, O.: Formation of phenol and carbonyls from the atmospheric reaction of OH radicals with benzene, *Phys. Chem. Chem. Phys.*, 8, 1205–1214, 2006.
- Berndt, T., Böge, O., Kind, I., and Rolle, W.: Reaction of NO₃ radicals with 1,3-cyclohexadiene, α -terpinene, and α -phellandrene: kinetics and products, *Ber. Bunsenges. Phys. Chem.*, 100, 462–469, 1996.
- Bignozzi, C., Maldotti, A., Chiorboli, C., Bartocci, C., and Carasiti, V.: Kinetics and mechanism of reactions between aromatic olefins and hydroxyl radicals, *Int. J. Chem. Kinet.*, 13, 1235–1242, 1981.
- Birdsall, A. W. and Elrod, M. J.: Comprehensive NO-dependent study of the products of the oxidation of atmospherically relevant aromatic compounds, *J. Phys. Chem. A*, 115, 5397–5407, 2011.
- Birdsall, A. W., Andreoni, J. F., and Elrod, M. J.: Investigation of the role of bicyclic peroxy radicals in the oxidation mechanism of toluene, *J. Phys. Chem. A*, 114, 10655–10663, 2010.
- Bloss, C., Wagner, V., Jenkin, M. E., Volkamer, R., Bloss, W. J., Lee, J. D., Heard, D. E., Wirtz, K., Martin-Reviejo, M., Rea, G., Wenger, J. C., and Pilling, M. J.: Development of a detailed chemical mechanism (MCMv3.1) for the atmospheric oxidation of aromatic hydrocarbons, *Atmos. Chem. Phys.*, 5, 641–664, <https://doi.org/10.5194/acp-5-641-2005>, 2005.
- Bouvier-Brown, N. C., Goldstein, A. H., Gilman, J. B., Kuster, W. C., and de Gouw, J. A.: In-situ ambient quantification of monoterpenes, sesquiterpenes, and related oxygenated compounds during BEARPEX 2007: implications for gas- and particle-phase chemistry, *Atmos. Chem. Phys.*, 9, 5505–5518, <https://doi.org/10.5194/acp-9-5505-2009>, 2009.
- Calvert, J. G., Atkinson, R., Becker, K. H., Kamens, R. M., Seinfeld, J. H., Wallington, T. J., and Yarwood, G.: Mechanisms of atmospheric oxidation of the aromatic hydrocarbons, Oxford University Press, Oxford, ISBN 0-19514628-X, 2002.
- Calvert, J. G., Mellouki, A., Orlando, J. J., Pilling, M. J., and Wallington, T. J.: The mechanisms of atmospheric oxidation of the oxygenates, Oxford University Press, Oxford, 2011.
- Cho, J., Roueintan, M., and Li, Z.: Kinetic and dynamic investigations of OH reaction with styrene, *J. Phys. Chem. A*, 118, 9460–9470, 2014.
- Clifford, G. M. and Wenger, J. C.: Rate coefficients for the gas-phase reaction of hydroxyl radicals with the dimethylbenzaldehydes, *Int. J. Chem. Kinet.*, 38, 563–569, 2006.
- Clifford, G., Thüner, L. P., Wenger, J., and Shallcross, D. E.: Kinetics of the gas-phase reactions of OH and NO₃ radicals with aromatic aldehydes, *J. Photoch. Photobio. A*, 176, 172–182, 2005.
- Coeur-Tourneur, C., Henry, F., Janquin, M.-A., and Brutier, L.: Gas-phase reaction of hydroxyl radicals with *m*-, *o*- and *p*-cresol, *Int. J. Chem. Kinet.*, 38, 553–562, 2006.
- Derwent, R. G., Jenkin, M. E., and Saunders, S. M.: Photochemical ozone creation potentials for a large number of reactive hydrocarbons under European conditions, *Atmos. Environ.*, 30, 181–199, 1996.
- Elrod, M. J.: Kinetics study of the aromatic bicyclic peroxy radical + NO reaction: overall rate constant and nitrate product yield measurements, *J. Phys. Chem. A*, 115, 8125–8130, 2011.
- Fan, J. and Zhang, R.: Atmospheric oxidation mechanism of *p*-xylene: a Density Functional Theory study, *J. Phys. Chem. A*, 110, 7728–7737, 2006.
- Fan, J. and Zhang, R.: Density Functional Theory study on OH-initiated atmospheric oxidation of *m*-xylene, *J. Phys. Chem. A*, 112, 4314–4323, 2008.
- Gentner, D. R., Jathar, S. H., Gordon, T. D., Bahreini, R., Day, D. A., El Haddad, I., Hayes, P. L., Pieber, S. M., Platt, S. M., de Gouw, J., Goldstein, A. H., Harley, R. A., Jimenez, J. L., Prévôt, A. S. H., and Robinson, A. L.: Review of urban secondary organic aerosol formation from gasoline and diesel motor vehicle emissions, *Environ. Sci. Technol.*, 51, 1074–1093, 2017.

- Glowacki, D. R., Wang, L., and Pilling, M. J.: Evidence of formation of bicyclic species in the early stages of atmospheric benzene oxidation, *J. Phys. Chem. A*, 113, 5385–5396, 2009.
- Haagen-Smit, A. J. and Fox, M. M.: Photochemical ozone formation with hydrocarbons and automobile exhaust, *J. Air Pollut. Control Assoc.*, 4, 105–109, 1954.
- Hallquist, M., Wenger, J. C., Baltensperger, U., Rudich, Y., Simpson, D., Claeys, M., Dommen, J., Donahue, N. M., George, C., Goldstein, A. H., Hamilton, J. F., Herrmann, H., Hoffmann, T., Iinuma, Y., Jang, M., Jenkin, M. E., Jimenez, J. L., Kiendler-Scharr, A., Maenhaut, W., McFiggans, G., Mentel, Th. F., Monod, A., Prévôt, A. S. H., Seinfeld, J. H., Surratt, J. D., Szmigielski, R., and Wildt, J.: The formation, properties and impact of secondary organic aerosol: current and emerging issues, *Atmos. Chem. Phys.*, 9, 5155–5236, <https://doi.org/10.5194/acp-9-5155-2009>, 2009.
- Harrison, J. C. and Wells, J. R.: Gas-phase chemistry of benzyl alcohol: reaction rate constants and products with OH radical and ozone, *Atmos. Environ.*, 43, 798–804, 2009.
- Hays, M. D., Geron, C. D., Linna, K. J., Smith, N. D., and Schauer, J. J.: Speciation of gas-phase and fine particle emissions from burning of foliar fuels, *Environ. Sci. Technol.*, 36, 2281–2295, 2002.
- Helmig, D., Balsley, B., Davis, K., Kuck, L. R., Jensen, M., Bogner, J., Smith, T., Arrieta, R. V., Rodríguez, R., and Birks, J. W.: Vertical profiling and determination of landscape fluxes of biogenic nonmethane hydrocarbons within the planetary boundary layer in the Peruvian Amazon, *J. Geophys. Res.-Atmos.*, 103, 25519–25532, 1998.
- Herbinet, O., Husson, B., Ferrari, M., Glaude, P. A., and Battin-Leclerc, F.: Low temperature oxidation of benzene and toluene in mixture with *n*-decane, *Proc. Combust. Inst.*, 34, 297–305, 2013.
- Huang, M., Wang, Z., Hao, L., and Zhang, W.: Density functional theory study on the mechanism of OH-initiated atmospheric photooxidation of ethylbenzene, *J. Molec. Struct.*, 944, 21–33, 2010.
- Huang, M., Wang, Z., Hao, L., and Zhang, W.: Theoretical investigation on the mechanism and kinetics of OH radical with *m*-xylene, *Comput. Theor. Chem.*, 965, 285–290, 2011.
- Iuga, C., Galano, A., and Vivier-Bunge, A.: Theoretical investigation of the OH-initiated oxidation of benzaldehyde in the troposphere, *Chem. Phys. Chem.*, 9, 1453–1459, 2008.
- IUPAC: Task Group on Atmospheric Chemical Kinetic Data Evaluation, http://iupac.pole-ether.fr/htdocs/datasheets/pdf/HOx_AROM2_HO_toluene.pdf (last access: September 2017), 2017a.
- IUPAC: Task Group on Atmospheric Chemical Kinetic Data Evaluation, http://iupac.pole-ether.fr/htdocs/datasheets/pdf/AROM_RAD1_HOC6H6_O2.pdf (last access: September 2017), 2017b.
- IUPAC: Task Group on Atmospheric Chemical Kinetic Data Evaluation, http://iupac.pole-ether.fr/htdocs/datasheets/pdf/AROM_RAD4_HOC7H8_O2.pdf (last access: September 2017), 2017c.
- Jenkin, M. E. and Clementshaw, K. C.: Ozone and other secondary photochemical pollutants: chemical processes governing their formation in the planetary boundary layer, *Atmos. Environ.*, 34, 2499–2527, 2000.
- Jenkin, M. E., Saunders, S. M., Wagner, V., and Pilling, M. J.: Protocol for the development of the Master Chemical Mechanism, MCM v3 (Part B): tropospheric degradation of aromatic volatile organic compounds, *Atmos. Chem. Phys.*, 3, 181–193, <https://doi.org/10.5194/acp-3-181-2003>, 2003.
- Jenkin, M. E., Hurley, M. D., and Wallington, T. J.: Investigation of the radical product channel of the $\text{CH}_3\text{C}(\text{O})\text{O}_2 + \text{HO}_2$ reaction in the gas phase, *Phys. Chem. Chem. Phys.*, 9, 3149–3162, 2007.
- Jenkin, M. E., Hurley, M. D., and Wallington, T. J.: Investigation of the radical product channel of the $\text{CH}_3\text{OCH}_2\text{O}_2 + \text{HO}_2$ reaction in the gas phase, *J. Phys. Chem. A*, 114, 408–416, 2010.
- Jenkin, M. E., Derwent, R. G., and Wallington, T. J.: Photochemical ozone creation potentials for volatile organic compounds: Rationalization and estimation, *Atmos. Environ.*, 163, 128–137, 2017.
- Jenkin, M. E., Valorso, R., Aumont, B., Rickard, A. R., and Wallington, T. J.: Estimation of rate coefficients and branching ratios for gas-phase reactions of OH with aliphatic organic compounds for use in automated mechanism construction, *Atmos. Chem. Phys.*, 18, 9297–9328, <https://doi.org/10.5194/acp-18-9297-2018>, 2018a.
- Jenkin, M. E., Valorso, R., Aumont, B., and Rickard, A. R.: Estimation of rate coefficients and branching ratios for reactions of organic peroxy radicals for use in automated mechanism construction, in preparation, 2018b.
- Klotz, B., Sørensen, S., Barnes, I., Becker, K. H., Etzkorn, T., Volkamer, R., Platt, U., Wirtz, K., and Martín-Reviejo, M.: Atmospheric oxidation of toluene in a large volume outdoor photoreactor: in situ determination of ring-retaining product yields, *J. Phys. Chem. A*, 102, 10289–10299, 1998.
- Kwok, E. S. C. and Atkinson R.: Estimation of hydroxyl radical reaction rate constants for gas-phase organic compounds using a structure-reactivity relationship: an update, *Atmos. Environ.*, 29, 1685–1695, 1995.
- Kwok, E. S. C., Aschmann, S. M., Atkinson, R., and Arey, J.: Products of the gas-phase reactions of *o*-, *m*- and *p*-xylene with the OH radical in the presence and absence of NO_x , *J. Chem. Soc.*, 93, 2847–2854, 1997.
- Lewis, A. C., Evans, M. J., Hopkins, J. R., Punjabi, S., Read, K. A., Purvis, R. M., Andrews, S. J., Moller, S. J., Carpenter, L. J., Lee, J. D., Rickard, A. R., Palmer, P. I., and Parrington, M.: The influence of biomass burning on the global distribution of selected non-methane organic compounds, *Atmos. Chem. Phys.*, 13, 851–867, <https://doi.org/10.5194/acp-13-851-2013>, 2013.
- Li, Y. and Wang, Y.: The atmospheric oxidation mechanism of 1,2,4-trimethylbenzene initiated by OH radicals, *Phys. Chem. Chem. Phys.*, 16, 17908–17917, 2014.
- Loison, J.-C., Rayez, M.-T., Rayez, J.-T., Gratien, A., Morajkar, P., Fittschen, P., and Villenave, E.: Gas-phase reaction of hydroxyl radical with hexamethylbenzene, *J. Phys. Chem. A*, 116, 12189–12197, 2012.
- Maleknia, S. D., Bell, T. L., and Adams, M. A.: PTR-MS analysis of reference and plant-emitted volatile organic compounds, *Int. J. Mass. Spectrom.*, 262, 203–210, 2007.
- Misztal, P. K., Owen, S. M., Guenther, A. B., Rasmussen, R., Geron, C., Harley, P., Phillips, G. J., Ryan, A., Edwards, D. P., Hewitt, C. N., Nemitz, E., Siong, J., Heal, M. R., and Cape, J. N.: Large estragole fluxes from oil palms in Borneo, *Atmos. Chem. Phys.*, 10, 4343–4358, <https://doi.org/10.5194/acp-10-4343-2010>, 2010.
- Misztal, P. K., Hewitt, C. N., Wildt, J., Blande, J. D., Eller, A. S. D., Fares, S., Gentner, D. R., Gilman, J. B., Graus, M., Greenberg, J., Guenther, A. B., Hansel, A., Harley, P., Huang, M., Jardine, K., Karl, T., Kaser, L., Keutsch, F. N., Kiendler-Scharr, A., Kleist, E., Lerner, B. M., Li, T., Mak, J., Nölscher, A. C., Schnitzhofer, R., Sinha, V., Thornton, B., Warneke, C., Wegener, F., Werner, C.,

- Williams, J., Worton, D. R., Yassaa, N., and Goldstein, A. H.: Atmospheric benzenoid emissions from plants rival those from fossil fuels, *Sci. Rep.*, 5, 12064, <https://doi.org/10.1038/srep12064>, 2015.
- Mousavipour, S. H. and Homayoon, Z.: Multichannel RRKM-TST and CVT rate constant calculations for reactions of CH_2OH or CH_3O with HO_2 , *J. Phys. Chem. A*, 115, 3291–3300, 2011.
- Nehr, S., Bohn, B., Fuchs, H., Hofzumahaus, A., and Wahner, A.: HO_2 formation from the $\text{OH} + \text{benzene}$ reaction in the presence of O_2 , *Phys. Chem. Chem. Phys.*, 13, 10699–10708, 2011.
- Nehr, S., Bohn, B., and Wahner, A.: Prompt HO_2 formation following the reaction of OH with aromatic compounds under atmospheric conditions, *J. Phys. Chem. A*, 116, 6015–6026, 2012.
- Nishino, N., Arey, J., and Atkinson, R.: Formation yields of glyoxal and methylglyoxal from the gas-phase OH radical-initiated reactions of toluene, xylenes, and trimethylbenzenes as a function of NO_2 concentration, *J. Phys. Chem. A*, 114, 10140–10147, 2010.
- Noda, J., Volkamer, R., and Molina, M. J.: Dealkylation of alkylbenzenes: a significant pathway in the toluene, o-, m-, and p-xylene + OH reaction, *J. Phys. Chem. A*, 113, 9658–9666, 2009.
- Odum, J. R., Jungkamp, T. P. W., Griffin, R. J., Forstner, H. J. L., Flagan, R. C., and Seinfeld, J. H.: Aromatics, reformulated gasoline, and atmospheric organic aerosol formation, *Environ. Sci. Technol.*, 31, 1890–1897, 1997.
- Olariu, R. I., Klotz, B., Barnes, I., Becker, K. H., and Mocanu, R.: FT-IR study of the ring-retaining products from the reaction of OH radicals with phenol, o-, m-, and p-cresol, *Atmos. Environ.*, 36, 3685–3697, 2002.
- Owen, S. M., Boissard, C., and Hewitt, C. N.: Volatile organic compounds (VOCs) emitted from 40 Mediterranean plant species: VOC speciation and extrapolation to habitat scale, *Atmos. Environ.*, 35, 5393–5409, 2001.
- Pan, S. and Wang, L.: Atmospheric oxidation mechanism of m-xylene initiated by OH radical, *J. Phys. Chem. A*, 118, 10778–10787, 2014.
- Passant, N. R.: Speciation of UK emissions of non-methane volatile organic compounds, AEA Technology Report ENV-0545, Culham, Abingdon, UK, 2002.
- Peeters, J., Vandenberk, S., Piessens, E., and Pultau, V.: H-atom abstraction in reactions of cyclic polyalkenes with OH , *Chemosphere*, 38, 1189–1195, 1999.
- Peeters, J., Boullart, W., Pultau, V., Vandenberk, S., and Vereecken, L.: Structure-activity relationship for the addition of OH to (poly)alkenes: site-specific and total rate constants, *J. Phys. Chem. A*, 111, 1618–1631, 2007.
- Perry, R. A., Atkinson, R., and Pitts, J. N.: Kinetics and mechanism of the gas phase reaction of OH radicals with methoxybenzene and o-cresol over the temperature range 299–435 K, *J. Phys. Chem.*, 81, 1607–1611, 1977.
- Platz, J., Nielsen, O. J., Wallington, T. J., Ball, J. C., Hurley, M. D., Straccia, A. M., Schneider, W. F., and Sehested, J.: Atmospheric chemistry of the phenoxy radical, *J. Phys. Chem. A*, 102, 7964–7974, 1998.
- Raoult, S., Rayez, M.-T., Rayez, J.-C., and Lesclaux, R.: Gas phase oxidation of benzene: Kinetics, thermochemistry and mechanism of initial steps, *Phys. Chem. Chem. Phys.*, 6, 2245–2253, 2004.
- Rickard, A. R., Wyche, K. P., Metzger, A., Monks, P. S., Ellis, A. M., Dommen, J., Baltensperger, U., Jenkin, M. E., and Pilling, M. J.: Gas phase precursors to anthropogenic secondary organic aerosol: using the Master Chemical Mechanism to probe detailed observations of 1,3,5-trimethylbenzene photo-oxidation, *Atmos. Environ.*, 44, 5423–5433, 2010.
- Saunders, S. M., Jenkin, M. E., Derwent, R. G., and Pilling, M. J.: Protocol for the development of the Master Chemical Mechanism, MCM v3 (Part A): tropospheric degradation of non-aromatic volatile organic compounds, *Atmos. Chem. Phys.*, 3, 161–180, <https://doi.org/10.5194/acp-3-161-2003>, 2003.
- Smith, D. F., McIver, C. D., and Kleindienst, T. E.: Primary product distribution from the reaction of hydroxyl radicals with toluene at ppb NO_x mixing ratios, *J. Atmos. Chem.*, 30, 209–228, 1998.
- Smith, D. F., Kleindienst, T. E., and McIver, C. D.: Primary product distributions from the reaction of OH with m-, p-xylene, 1,2,4- and 1,3,5-trimethyl benzene, *J. Atmos. Chem.*, 34, 339–364, 1999.
- Suh, I., Zhang, D., Zhang, R., Molina, L. T., and Molina, M. J.: Theoretical study of OH addition reaction to toluene, *Chem. Phys. Lett.*, 364, 454–462, 2002.
- Suh, I., Zhang, R., Molina, L. T., and Molina, M. J.: Oxidation mechanism of aromatic peroxy and bicyclic radicals from OH -toluene reactions, *J. Am. Chem. Soc.*, 125, 12655–12665, 2003.
- Tao, Z. and Li, Z.: A kinetics study on reactions of $\text{C}_6\text{H}_5\text{O}$ with $\text{C}_6\text{H}_5\text{O}$ and O_3 at 298 K, *Int. J. Chem. Kinetics*, 31, 65–72, 1999.
- Thiault, G., Mellouki, A., and Le Bras, G.: Kinetics of gas phase reactions of OH and Cl with aromatic aldehydes, *Phys. Chem. Chem. Phys.*, 4, 2194–2199, 2002.
- Tuazon, E., Arey, J., Atkinson, R., and Aschmann, S.: Gas-phase reactions of vinylpyridine and styrene with OH and NO_3 radicals and O_3 , *Environ. Sci. Technol.*, 27, 1832–1841, 1993.
- Ulman, M., Bielawska, K., Łozowicka, B., Heimann, M., Kesselmeier, J., Schebeske, G., Katryński, K. S., and Chilmonczyk, Z.: Determination of volatile organic compounds (VOCs) in the atmosphere over central Siberian forest and southern part of European Taiga in Russia, *Chem. Anal.*, 52, 435–451, 2007.
- Vereecken, L.: Reaction mechanisms for the atmospheric oxidation of monocyclic aromatic compounds, in: *Advances in Atmospheric Chemistry*, edited by: Barker, J. R., Allison, S., and Wallington, T. J., Vol. 2, accepted, 2018a.
- Vereecken, L.: Interactive comment on “Estimation of rate coefficients and branching ratios for gas-phase reactions of OH with aromatic organic compounds for use in automated mechanism construction” by Michael E. Jenkin et al., *Atmos. Chem. Phys. Discuss.*, <https://doi.org/10.5194/acp-2018-146-SC1>, 2018b.
- Volkamer, R., Platt, U., and Wirtz, K.: Primary and secondary glyoxal formation from aromatics: experimental evidence for the bicycloalkyl-radical pathway from benzene, toluene and p-xylene, *J. Phys. Chem. A*, 105, 7865–7874, 2001.
- Volkamer, R., Klotz, B., Barnes, I., Imamura, T., Wirtz, K., Washida, N., Becker, K. H., and Platt, U.: OH -initiated oxidation of benzene – Part I. Phenol formation under atmospheric conditions, *Phys. Chem. Chem. Phys.*, 4, 1598–1610, 2002.
- Wang, L., Arey, J., and Atkinson, R.: Kinetics and products of photolysis and reaction with OH radicals of a series of aromatic carbonyl compounds, *Environ. Sci. Technol.*, 40, 5465–5471, 2006.
- Went, F. W.: Blue hazes in the atmosphere, *Nature*, 187, 641–645, 1960.

- Wu, R., Pan, S., Li, Y., and Wang, L.: Atmospheric oxidation mechanism of toluene, *J. Phys. Chem. A*, 118, 4533–4547, 2014.
- Yu, J. Z. and Jeffries, H. E.: Atmospheric photooxidation of alkylbenzenes, 2. Evidence for formation of epoxide intermediates, *Atmos. Environ.*, 31, 2281–2287, 1997.